CHALMERS
UNIVERSITY OF TECHNOLOGY

Study of Design Parameters influence on the Fatigue Life of Riveted Joints

Master's thesis in Applied Mechanics

Ingrid Lövgren

Department of Industrial and Materials Science
CHALMERS UNIVERSITY OF TECHNOLOGY
Gothenburg, Sweden 2018

MASTER'S THESIS IN APPLIED MECHANICS

Study of Design Parameters influence on the Fatigue Life of Riveted Joints

Ingrid Lövgren

Department of Industrial and Materials Science
Division of Material and Computational Mechanics
CHALMERS UNIVERSITY OF TECHNOLOGY
Göteborg, Sweden 2018

Study of Design Parameters influence on the Fatigue Life of Riveted Joints

Ingrid Lövgren

Master's Thesis
ISSN 1652-8557
Department of Industrial and Materials Science
Division of Material and Computational Mechanics
Chalmers University of Technology
SE-412 96 Göteborg
Sweden
Telephone: + 46 (0)31-772 1000

Cover:
Fractured riveted joint after fatigue loading

Chalmers reproservice / Department of Industrial and Materials Science
Göteborg, Sweden 2018-12-13

Study of Design Parameters influence on the Fatigue Life of Riveted Joints
Master's thesis in Applied Mechanics
Ingrid Lövgren
Department of Industrial and Materials Science
Division of Material and Computational Mechanics
Chalmers University of Technology

Abstract

The aim of this study is to identify and investigate design parameters influence on the fatigue life of riveted joints. This to allow Volvo Group to fully utilize what the riveted joint has to offer.

In the literature review many design parameters were identified as influencing the fatigue life of riveted joints. Some design parameters were chosen to be further investigated: hole geometry, hole treatment, plate material and rivet head design. Numerical and experimental investigations were conducted on a single riveted lap joint consisting of 15 mm solid rivets and 5 mm thick plates. A simulation of the riveting process was performed together with a simplified shear loading simulation of a lap joint. The numerical simulations were found to correspond well to experimental data such as deformation in shaped rivet head, stress fields, crack initiation and fretting location. Very few samples were investigated experimentally, limiting the statistically robustness of the results, but trends could still be observed.

During the literature review three features were identified as necessary to consider to obtain a strong and robust riveted joint: the filling of the hole, the residual stress fields and the load transfer path. Furthermore, the most influential design parameter was identified as the riveting force. During numerical and experimental studies it was observed that the hole geometry influences residual stress fields and crack initiation. It was also indicated that the most detrimental hole geometry is the straight hole geometry, as residual hoop tension was observed after the riveting. Incomplete filling of the holes resulted in small voids, maximum of 1.0 x 0.5 mm, between rivet and plate interface. No detrimental effect of these voids was observed. In this study, large beneficial effects of hole treatments could not be confirmed at the investigated medium high load level. The shear loading simulation shows that the highest stress range occurs at the plate interface which corresponded to the crack initiation location observed during experiments. During the experiments it was further observed that the fracture mode corresponds to the load level. It is therefore concluded that to obtain a strong riveted joint with a long fatigue life a balance between design parameters is then needed.

Key words: Fatigue life, Riveted joint, Chassis, Parameters

Contents

Preface

This study has been performed for Volvo Group at the product development division Volvo Group Trucks Technology (GTT) CVD at DC group Fuel Supply, Battery Box & Energy Storage System. It has been performed to increase Volvo Group's knowledge about riveted joints to allow more robust products and best practice design formulations.

This study has been carried out with Lead Analyst Sébastien Ragot as the supervisor at Volvo Group Truck Technology and Professor Magnus Ekh as supervisor at Chalmers University of Technology. All tests have been carried out in A-hallen at Volvo GTT. This study would not have been possible without all the help and support I have received from different people at Volvo GTT. I would like to thank Tobias Andersson and Yogesh Ramachandra for all help and support regarding the numerical simulations. I would also like to thank Sigge Klintman at SSAB for providing material to the experiments and Andreas Lindblom together with Ebbe Svensson for the support and help of creating all test specimens. I would further like to thank Mats Palmgren for running the test rig during the fatigue life experiments and Matthias Widmark for providing support during evaluation of all test specimens.

Finally, I would like to thank Sebastien Ragot and Magnus Ekh for the continued support through this study.

Göteborg 2018-12-13

Ingrid Lövgren

Notations

Roman letters

A_{rivet}	Area of cross second of rivet shank after riveting
A_{plate}	Area of cross section of plate
D	Nominal diameter of shank before riveting
D_{drill}	Diameter of drill bit
D_e	Nominal diameter of the rivet shank and hole after riveting
D_{fixed}	Diameter of stamping tool, fixed die
D_h	Nominal diameter of hole before riveting
D_{max}	Maximum diameter of hole
D_{min}	Minimum diameter of hole
$D_{mandrel}$	Maximum mandrel diameter
D_{punch}	Diameter of the stamping tool, punch
D_s	Maximum shaped rivet head diameter
E	Young's modulus
f	Frequency
I	Stress transfer
I_J	Stress transfer estimated from Jennfors, P. (1993)
H	Length of the rivet shank before riveting
$H_{s,1}$	Maximum hight of shaped rivet head
$H_{s,2}$	Edge height of shaped rivet head
L_{bottom}	Length of bottom hole wall section
L_{free}	Free length of the rivet shank
L_{plate}	Length of plate
$L_{plate,load}$	Distance from riveted joint centre to applied loading
L_{top}	Length of top hole wall section
m	Estimated true mass of the FE-model
m_{scaled}	Scaled mass used for dynamic explicit calculations
N	Load cycles to failure
R	Ratio of applied minimum and maximum cyclic load
S	Applied load
S_{max}	Maximum applied load amplitude
$S_{max,Rig}$	Maximum applied load capacity of the tensile test rig
$S_{max,L}$	Applied load amplitude for low load
$S_{max,M}$	Applied load amplitude for medium load
$S_{max,H}$	Applied load amplitude for high load
S_{min}	Minimum applied load amplitude
t	Thickness of plate
t_{inc}	Time increment
t_{tot}	Total simulated time
u_x	Displacement in x- direction
u_y	Displacement in y- direction
u_z	Displacement in z- direction
w	Width of plate

Greek letters

ε	Strain
ε_e	Elastic strain
ε_p	Plastic strain
θ	Angle of hole wall
σ	Stress
σ_{plate}	Nominal stress in plate
σ_u	Ultimate tensile strength
τ_{rivet}	Nominal shear in rivet

Acronyms and terms

ABAQUS	Finite element software
ALE	Arbitrary Lagrange – Eulerian. Mesh adaptive algorithm in ABAQUS
ANSA	Preprocessor software
Factory rivet head	Original rivet head
FE	Finite Element
Fixed die	Stationary die during riveting or stamping
Free length	Rivet shank length protruding outside plates
Hammer die	Moving die during riveting
NLGEOM	Nonlinear geometry. ABAQUS parameter that take nonlinear geometrical behaviour into account.
Plate 1	Plate located below factory rivet head
Plate 2	Plate located below shaped rivet head
RF	Riveting force used in production of Volvo Group trucks
Riveting force	Maximum force applied during riveting
RS	Riveting speed available during assembly of specimens
Shank	Body of rivet
Shaped rivet head	Rivet head created during riveting
TR	Technical report
TID	Test ID for experimental specimens

1 Introduction

Optimization of products has always been of interest for society and will always be of interest as different goals are desired at different times. The reason for optimization and the goal to be reached for industries have changed over the last years towards cost effectiveness and more environmental considerations. This is highly relevant for the truck industry where optimization towards energy efficiency has taken place. One way to reduce energy consumption during truck utilization is to reduce the weight of the vehicle itself. Knowledge about what impact every aspect and component of the vehicle is therefore necessary. This study looks at what and how riveted joints are influenced by design parameters.

1.1 Background

Volvo Group [Volvo Group (2018)] is a leading company on the global commercial vehicle market. Their vehicles have changed and will continue to change to accommodate new requirements and demands. The evolving requirements and demands on the trucks require constant new designs, which put new loads such as stresses and strains on the frame ladder. The frame ladder on a Volvo Goup truck consists of the frame sides and cross members as shown in Figure 1. When joints in the frame are subjected to high shear loads bolts are exchanged to rivets. The cross members are a part subjected to high shear loads and is therefore constructed with riveted joints. Deeper knowledge about the riveted joint behavior is needed at Volvo Group to fully utilize everything that the riveted joint has to offer. This study therefore aims to deepen the knowledge about parameter impact on fatigue life of riveted joints to improve Volvo Groups's technical requirements (TR) [TR Rivet (2017)].

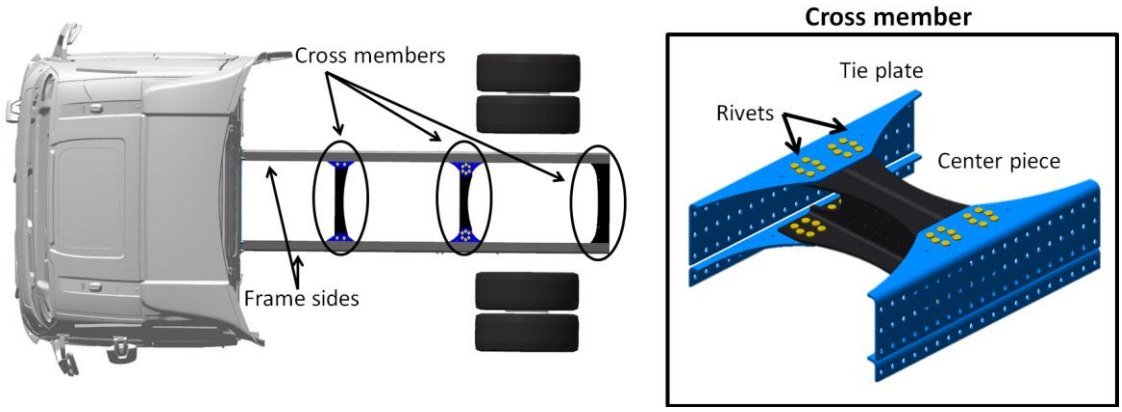

Figure 1 Chassis and cross member overview.

1.2 Objective

The objective of this study is to increase Volvo Groups's knowledge of what parameters influence the fatigue life of riveted joints by

- Identify possible parameters that can impact fatigue life of riveted joints by performing a literature review.
- Identify how previous simulations and experiments of riveted joints have been conducted.
- Create a numerical simulation of a riveted joint that can be used to evaluate the impact of different design parameters on fatigue life.
- Conduct experiments to compliment and validate the numerical simulations.
- Provide material for more in depth design and construction recommendations for the design of riveted joints at Volvo Group.
- Establish recommendations for future work regarding which parameters to investigate for fatigue life improvements.

1.3 Limitations

This study will encompass one riveted lap joint to simplify the simulations and experiments. The fatigue life experiments will be performed with a uniaxial test machine to further simplify and focus on the riveted joint itself. The loading in experiments and simulations will be estimated from vehicle service loads and inspired by previous works. The results in this study will provide indications on what parameters may influence a riveted joints fatigue life.

2 Theory and literature review

This section aims to give a basic understanding of what a rivet is and how the riveting process is conducted. Investigated literature for this report comes from either earlier work by Volvo Group or is published by the aviation industry, where many in depth studies have been conducted on riveted joints.

2.1 Riveted joints

Riveted joints are widely used in buildings, aircrafts and automotive industry to permanently hold parts together. The rivet itself is designed for the desired use. It can be completely solid for reliability and safety or designed with a partly hollow core to reduce needed riveting force. The rivet can also be designed as a blind rivet to be able to rivet parts together that only have access on one side of the hole. Many more varieties exist but the basic idea of a riveted joint is the same regardless of how the rivet is designed. The rivet shall plastically deform and fill a hole and create a secondary head to permanently fix parts together. Rivets in automotive and aircraft industry are mainly solid rivets as durability, reliability and safety are important considerations. Solid rivets that will be used in this study are shown in Figure 2 with round and flat rivet heads.

Figure 2: Solid rivets with round and flat head.

The rivet, before riveting, consists of a rivet head called the factory rivet head and a shank with diameter, D as shown in Figure 3. The shank protrudes from the hole a certain distance, in this study referred to as the free length, L_{free}. In this study the plate below the factory head is called plate 1 while the other plate is referred to as plate 2. The clearance between rivet shank and plates is called the radial clearance.

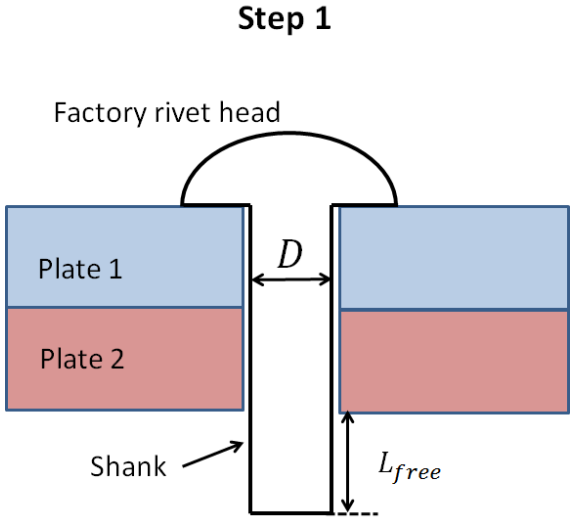

Figure 3 Riveted joint terms before riveting. Step 1 in the riveting process.

After the rivet is inserted in the premade hole the riveting process is conducted as shown in Figure 4. The rivet shank expands to fill the hole and cover the hole at both ends to permanently lock the plates together. The complete riveting process is performing in the following steps

1. The rivet is placed in a premade hole. The plates are fixed in some way to prevent undesired movements.
2. The fixed die is placed on top of the factory rivet head to hold the rivet in place.
3. The hammer die engage until desired riveting force has been reached. The hammer die is first displacement controlled, then force controlled.
4. When the desired riveting force has been reached the force is held constant to allow the material to fully deform.
5. All riveting dies are removed and the material experience spring back due to the material elasticity.

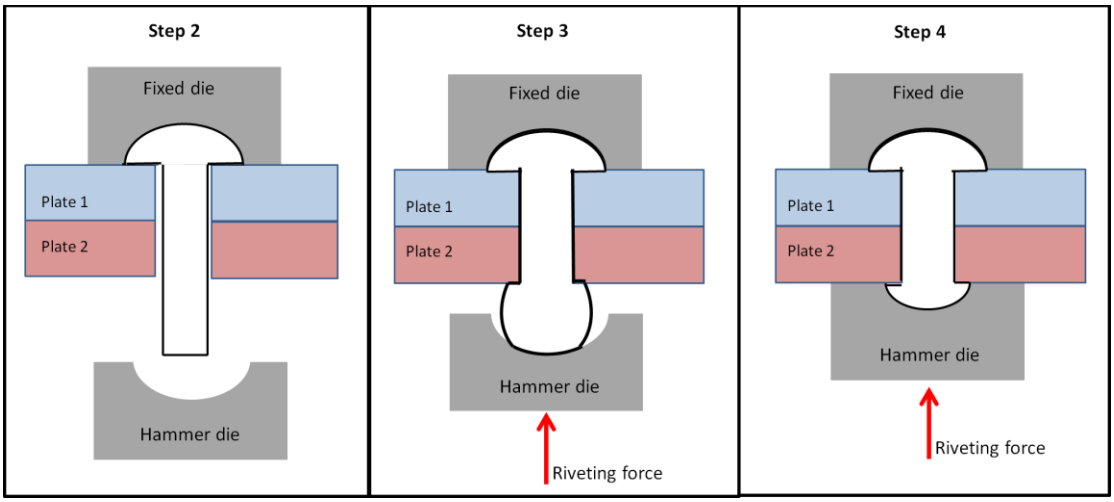

Figure 4 Riveting process. Step 2 to step 4.

During the riveting process the free length of the shank contributes to the filling of the hole and the geometry of the shaped rivet head, shown in Figure 5. In most cases the shaped rivet head is slightly smaller in diameter than the factory rivet head as the free length is limited to reduce the risk for buckling. The plate interface is the surface area between plate 1 and plate 2.

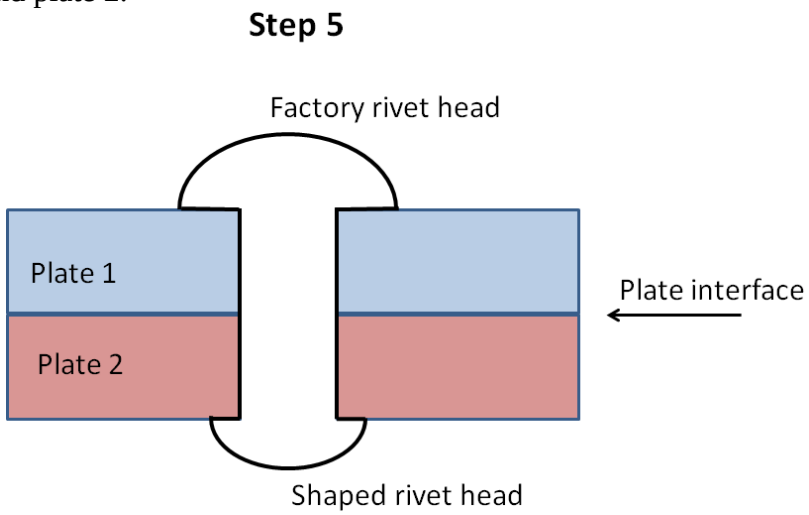

Figure 5 Riveted joint terms after riveting, step 5 in the riveting process.

Sufficient squeeze force between the factory rivet head and the shaped rivet head is needed to form a tight and durable riveted joint. The rivet shank also needs to expand to fully fill hole.

During the riveting process residual stresses are obtained in the rivet and the plates due to the plasticity that occur. The axial residual stresses are small compared to the radial and circumferential residual stresses that are of similar order of magnitude [Baha II, S., Hesebeck, O. (2010)].

2.1.1 Loading

A rivet is better that a bolt or a screw of withstanding shear loads. This, as the rivet completely fills the hole and therefore prevents hole deformations and sliding of the plates during shear loading. A lap joint subjected to shear loading respective axial loading is shown in Figure 6.

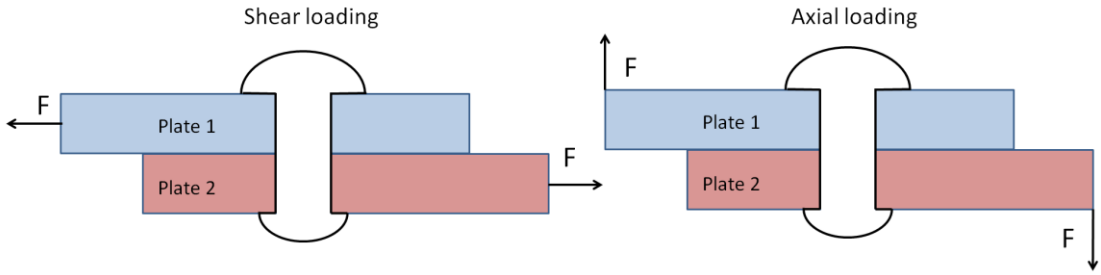

Figure 6 Shear and axial loading of riveted joint

The residual stresses obtained after the riveting process are important to consider for obtaining a robust riveted joint with a long fatigue life. The residual stresses are expressed in cylindrical coordinates due to the revolving aspect of the riveted joint., axial, hoop and radial direction as shown in Figure 7. The axial residual stress provides the residual squeeze stress that holds the two plates together. With a high residual squeeze stress the friction at the plate interface will increase and more of the load will be transferred through friction instead of through the rivet itself. Residual hoop stress is the circumferential residual stress that is obtained in the hole wall by the pressure from the rivet shank during the riveting process. Residual compressive hoop stress is beneficial to the fatigue life as the compressive stresses will delay crack initiation and slow down crack propagation [Dowling, N. E. (2013)]. Compressive hoop stress can be created by plasticising of the hole wall and then allow the spring back around the hole to compress the plasticised material. The residual radial stress is created by the pressure that the rivet shank exert on the hole wall.

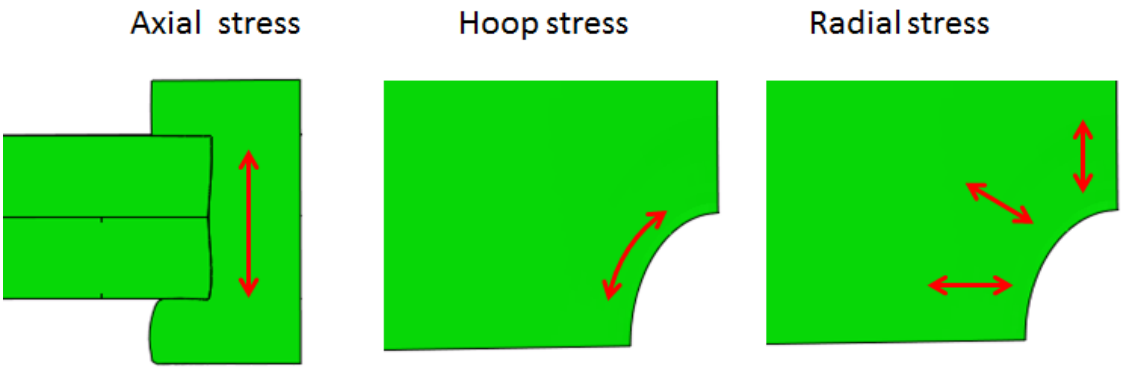

Figure 7 Squeeze stress and hoop stress.

During fatigue loading fretting, as a kind of corrosion damage, occurs due to wear between surfaces. The fretting creates debris, which can act as stress concentration points and induce fatigue related cracks. With a high contact pressure between parts the fretting can be reduced. During fatigue loading of a riveted joint the mean stress, σ_m, and the stress amplitude, σ_a, is of importance, Figure 8. The mean stress is the nominal stress experienced in a point before fatigue loading is applied. The stress amplitude is the stress range that the same point experienced during loading. The stress amplitude is calculated as

$$\sigma_a = \frac{\Delta\sigma}{2} = \frac{\sigma_{max} - \sigma_{min}}{2} \quad (1)$$

Where σ_{max} is the maximum stress experienced in the investigated point and σ_{min} is the minimum stress experienced in the same point. The residual stress obtained during the riveting process contributes, often a large part, to mean stress of the riveted joint. The stress amplitude is influenced by the applied fatigue loading of the joint and the mean stress.

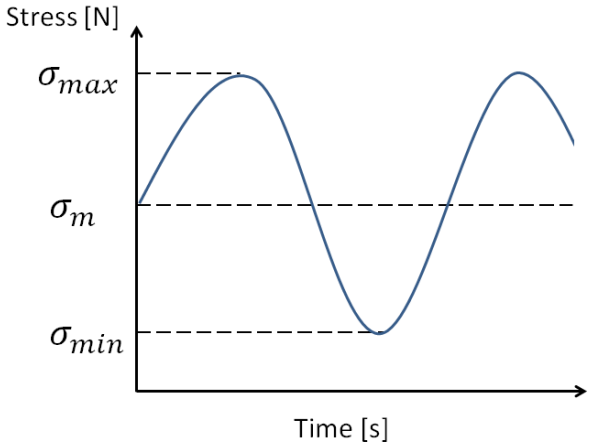

Figure 8 Fatigue loading terms.

A high mean stress and large stress amplitude will decrease the fatigue life. The equivalent stress can then be used to estimate the combined stress response in in the investigated point. This take into consideration the damage that the mean stress and stress amplitude has on fatigue life. One way to quantify the equivalent stress is with Smith Watson Topper equation

$$\sigma_{eq} = \sqrt{\sigma_{max} * \sigma_a} \quad (2)$$

See Dowling, N. E. (2013) for further information about fatigue behaviour.

2.2 Design parameters for a riveted joint

In this section parameters that influence the fatigue life of riveted joints are identified and stated. Studies related to the aviation industry have thin plates, about a thickness of 2 mm $\leq t \leq$ 6 mm, with holes created by drilling. In studies performed at Volvo Group the plates are thicker, about 5 mm $\leq t \leq$ 8 mm, and the holes are created using stamping, water cutting or plasma cutting. Parameters and attributes from both aviation industry and Volvo Group will be included in the study even as dimensions and hole penetration method vary between the industries.

Many parameters influence the response of a riveted joint. This literature study will focus only on design parameters influence on the fatigue life of riveted joint. Design parameters are defined as parameters that can be influenced by the engineer during design of the riveted joint or the operator during the riveting process. Many design parameters were found that could influence the riveted joint

- Rivet head design
- Rivet and plate material
- Surface treatment
- Radial clearance between rivet and plates
- Hole penetration method
- Hole treatment
- Hole geometry
- Shaped rivet head dimensions
- Riveting force
- Riveting speed

The following sections will explain the different design parameters influence on the riveted joint.

2.2.1 Rivet head design

Studies show that with increased amount of material added at the center of the riveted joint the filling of the hole and therefore also the fatigue life can be increased. Material can be guided to the center of the riveted joint by the design of the riveted head.

Improved filling were observed with addition of a compensator to a round head rivet for Skorupa, M., Skorupa, A., Machniewicz, T. et al. (2010). While Fuiorea, I., Bartis, D., Nedelcu, R. (2009) identified improved filling with a countersunk factory head compared to the round head design. Both head designs are shown in Figure 9.

Fuiorea, I., Bartis, D., Nedelcu, R. (2009) also showed that the ultimate fatigue strength was significantly increased with the use of a countersunk head compared to a round head rivet. It was indicated that the increased pressure of the round head on plate 1 resulted in larger, undesired, plate deformations (plate thickness of 3.8 mm $\leq t$ 5.25 mm) lead to the decreased of the ultimate fatigue strength.

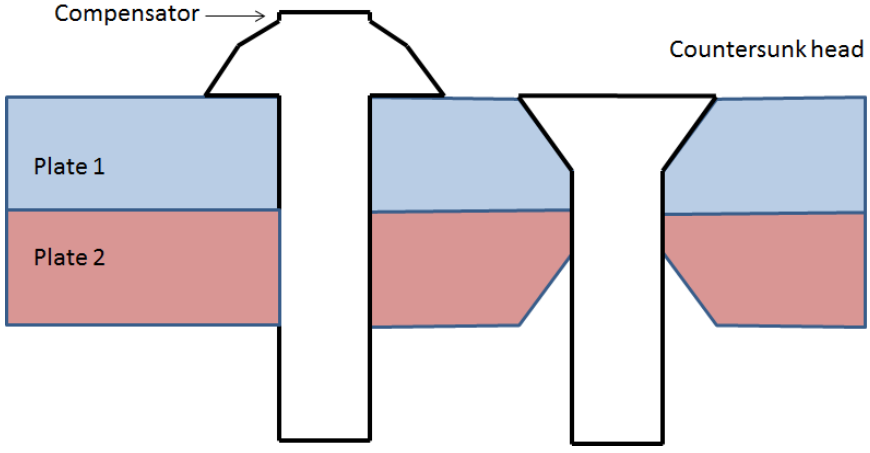

Figure 9 Round rivet head with compensator and countersunk rivet head.

2.2.2 Rivet and plate material

Studies show that the hardness of the rivet material influences the fatigue life. It is also shown that the combination of plate and rivet material properties influence the behavior of the riveted joint.

Heat treatment to soften the rivet material, annealing, resulted for Jennfors, P. (1993) in a longer fatigue life of the riveted joint compared to no heat treated rivet. The rivet material and the heat treatment of the rivets are important as the rivets need to be soft enough to deform before the plate does. With heat treatment and the subsequently decrease of hardness of the rivet the fatigue life was almost doubled in Sandström, B. (1993) as a result of the improved filling.

Lacroix, D. (2016) showed that a harder rivet material decreased the filling of the hole. Desired filling could then be reached if the harder rivet material was accompanied by a higher riveting force. Baha II, S., Hesebeck, O. (2010) indicate that the plate material spring back needs to be more than the rivet material spring back to obtain sufficient residual squeeze stress of the joint.

2.2.3 Surface treatment

Studies show that the surface treatment of the plates can influence the friction at the plate interface and therefore also influence the load transfer path in the riveted joint. Surface treatment of rivet and plate also influence the amount of fretting debris that can be created during fatigue loading.

Abdulwahab, F. (2009) indicates that the friction at the plate interface influenced the fatigue life. With increased friction they obtained a better fatigue life of the riveted joint. Skorupa, M., Skorupa, A., Machniewicz, T. et al. (2016) investigated the friction effect on the fatigue a life more in depth. They concluded that a lower friction at the plate interface had a beneficial effect on fatigue life as it limited the fretting debris and evened the load distribution between several riveted joints. They also obtained indications that a reduced friction was detrimental when the riveted joint was load was subjected to high loads.

Lacroix, D. (2016) showed that the risk with surface treatment such as paint or corrosion treatment of the rivet increased particles as the treatment of the rivet cracked during the riveting process. With the increased amount of particles the risk for fretting and additional stress concentrations points that can initiate fatigue cracks increase.

2.2.4 Radial clearance

Studies show that the radial clearance influences the fatigue life. The optimal radial clearance depends on the rivet and plate material in combination with the used riveting force.

Jennfors, P. (1993) concluded that the radial clearance influences the hole filling and the riveted joints strength. With a larger hole more material can fit inside and the strength of the joint increase. The clearance between rivet shank and hole walls needs to be adjusted to provide good filling with the chosen rivet material. A softer rivet will need larger clearance than a harder rivet to reach the same properties. Also indicated in the study was that the radial clearance should be kept as small as possible

for an increased fatigue life. Baha II, S., Hesebeck, O. (2010) confirmed that the radial clearance influenced the riveted joint strength.
Additionally, Skorupa, M., Machniewicz, T, Skorupa, A. et al. (2015) showed that with increased hole diameter tolerances the deviation in fatigue life prediction increased.

Fuiorea, I., Bartis, D., Nedelcu, R. (2009) showed that for high loading a thicker riveted joint resulted in longer fatigue life while, at low loads, the riveted joint thickness decreased in importance.

2.2.5 Hole penetration method

The mean stress in the riveted joint and the surface roughness are two properties that influence fatigue life [Dowling, N. E. (2013)]. The choice of hole penetration method influences surface roughness in hole walls, the residual stress field around the hole and the hole wall geometry. As such, the hole penetration method should be an important design parameter for fatigue life estimations.

During the literature review it was found that the hole penetration method was disregarded in studies published by the aviation industry [cf. Lipski, A. (2012)]. The reason why the hole penetration method was disregarded could be that the aviation industry uses drilled hole. Drilling produce a smooth hole walls and has a limited influence around the hole. No study could be found at Volvo Group that investigated the influence of the hole penetration method. A schematic representations of hole wall geometry for different hole penetration methods are shown in Figure 10.

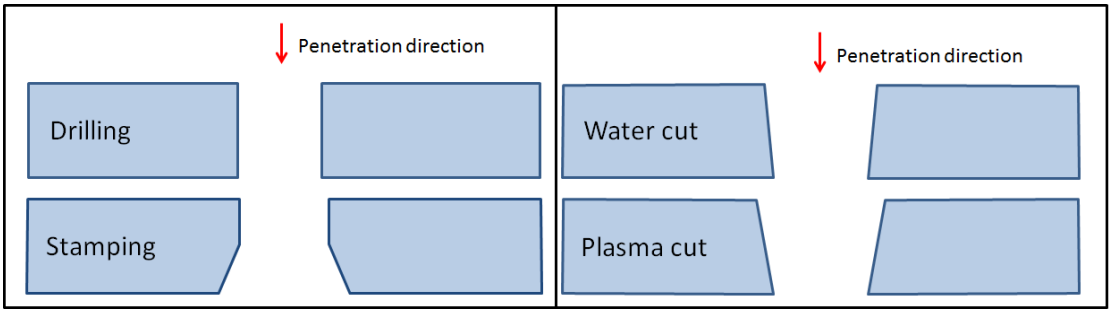

Figure 10 Hole wall geometry for different hole penetration methods.

Drilling is a hole penetration method that creates straight and smooth hole walls and has a minimal influence on the residual stress field around the hole. A stamped hole is created using a punch and a fixed die as shown in Figure 11. The punch diameter has to be smaller than the fixed die diameter, $D_{punch} < D_{fixed}$, to allow material to be removed without problems. The difference in diameter results in a conical wall section close to the fixed die. Stamping produce rougher hole walls than drilling and a small residual stress field influence in the plate.

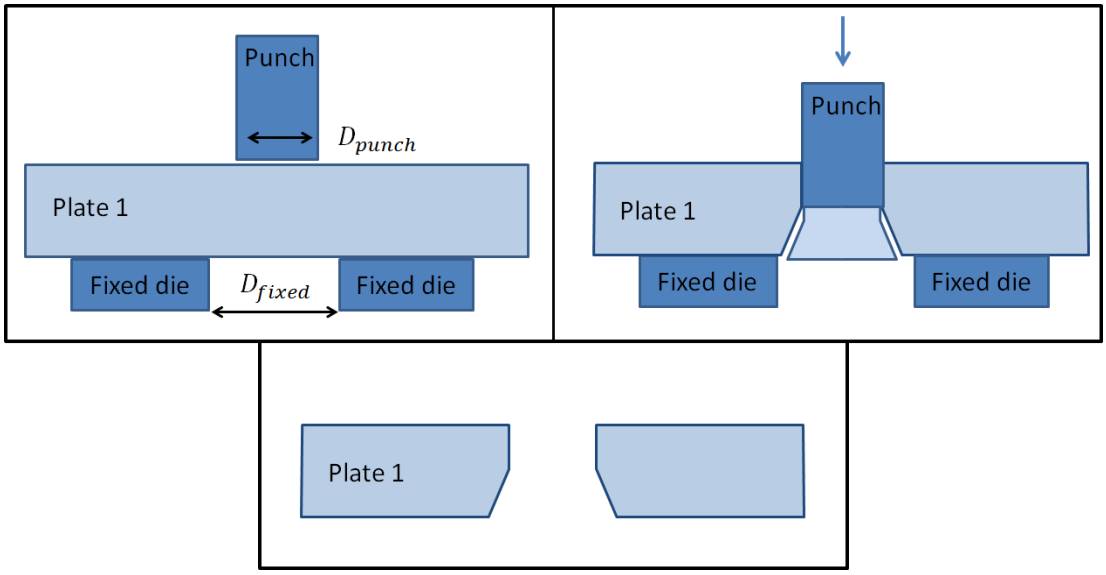

Figure 11 Stamping process and resulting hole geometry

The wall angles created during stamping can be reduced by using a pre punch method. A first, smaller hole, is punched, followed by a second stamping at the final diameter. Removal of material in the first punch allow the decrease in clearance between fixed die and punch when making the final hole, and therefore a straighter hole wall is created.

Water cutting produce smooth and almost straight walls with a small influence on the residual stress field. Plasma cutting often create slightly more angled walls than water cutting with a rather good surface but a larger influence on the residual stress field.

2.2.6 Hole treatment

Studies shows that the hole can be treated in different ways to mitigate undesired properties, such as surface roughness, angled hole walls or high hoop tension, that arose from the chosen hole penetration method.

Lipski, A. (2012) proved that with smooth hole walls the fatigue life was increased for a riveted joint. It was also proven that with cold working of the hole walls the fatigue life was increased even more. The effect on the fatigue life of the riveted joint for both methods increased with decreasing fatigue load, which would be as expected as cold forming induce compressive hoop stresses and polishing reduce stress concentrations.

Cold forming of hole walls was accomplished with the use of a mandrel for Lipski, A (2012). Cold forming by mandrel can change the hole geometry but mainly influence the residual stress in the hole walls. A mandrel with a diameter, $D_{mandrel}$, is pushed through a hole with a smaller diameter, D_{max}. When the mandrel is pressed through the hole the hole walls experienced strain hardening. After removal of the mandrel comparative compressive residual stresses are obtained in the hole walls as results of the elastic spring back of the plate. The cold forming process with use of a mandrel is illustrated in Figure 12.

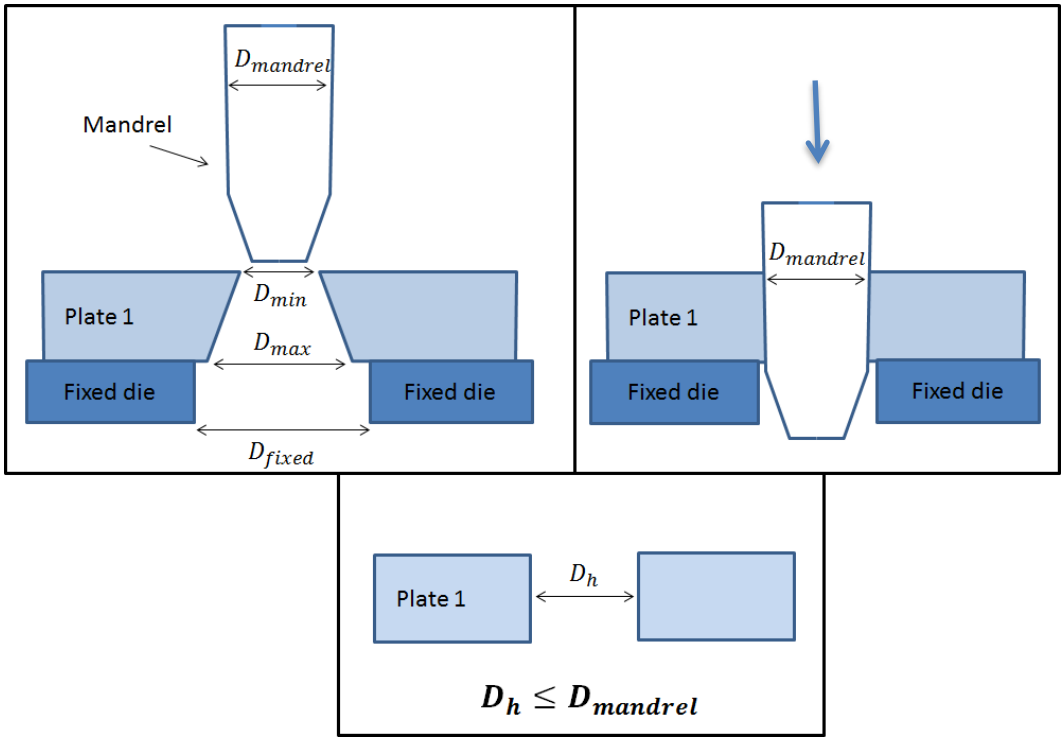

Figure 12 Schematic figure of cold forming process using a mandrel $D_{fixed} > D_{mandrel} \geq D_{max}$

The sizing degree is obtained as $k = \frac{D_h - D_{mandrel}}{D_{mandrel}} * 100\%$ were D_h is the nominal hole size after the removal of the mandrel. The optimal sizing degree for Lipski, A. (2012) was $k = \frac{3}{5}$ %, higher sizing degee resulted in larger variation in the fatigue life, not smaller.

Elajrami, M., Miloud, R., Milouki, H., et al. (2016) also investigated cold forming by mandrel but expanded the investigation by looking at double penetration of the mandrel. During double penetration the mandrel is first punched through the hole as shown in Figure 12, and then the mandrel is punched through the hole in the opposite direction. It was proven that the fatigue life was significantly improved for both single and double penetration. For single penetration the fatigue life was extended up to 7 times and for double penetration up to 11 times.

2.2.7 Hole geometry

Studies indicates that the filling of the hole is important for the fatigue life [cf. Sandström, B. (1993)]. Different hole penetration methods and different material hardnesses can possibly influence the hole filling.

Hole wall geometry may differ depending on the hole penetration method. If, for example, stamping, plasma cutting or water cutting is used the hole geometry becomes conically shaped. When combining two or more plates that have conical holes the hole geometry for the riveted joint can be varied. Convex, hourglass or stacked shapes of the hole can be created depending on how the plates are placed before the riveting process, Figure 13. The hole geometries may influence the hole filling. Abdulwahab, F. (2009) indicates that if the rivet is not concentrically riveted

the scatter during fatigue life evaluation is increased. If a non-concentrically riveted joint influence the fatigue life there is a possibility that different hole geometries may also influence the fatigue life.

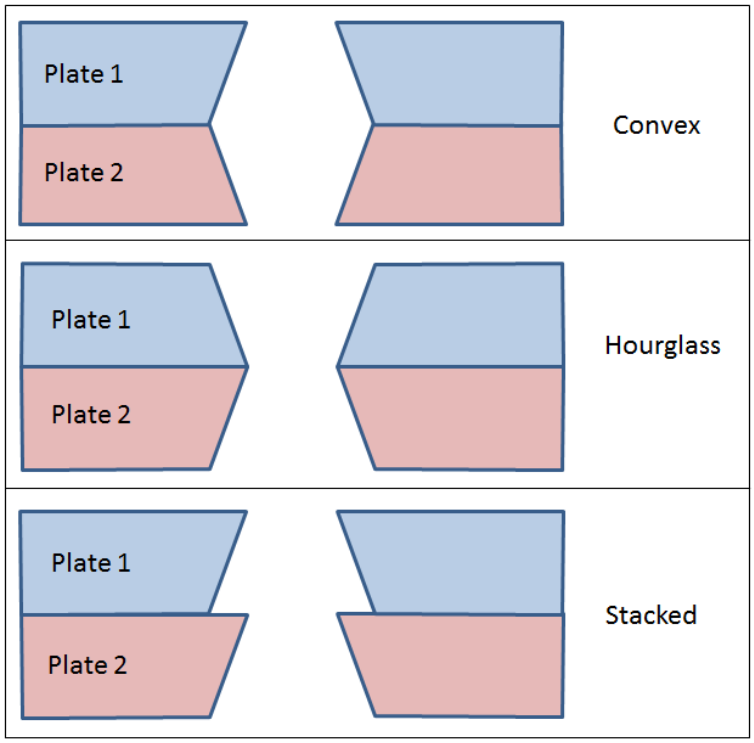

Figure 13 Different hole geometries.

2.2.8 Shaped rivet head dimensions

Studies show that the shaped rivet head geometry depends mainly on the design of the hammer die, the amount of free length of the shank and the riveting force. The shaped rivet head geometry seems often to be used to verify numerical simulations of the riveting process.

Lacroix, D. (2016) showed that with harder rivet material an increased riveting force was needed to form the same sized of the shaped rivet head as a softer counterpart. The free length needed to consist of enough material to properly fill the hole and create as large shaped head as desired. Increased shaped rivet head diameter, D_s in Figure 14, improved the possibility to withstand an increased axial loading. With a long free length the rivet shank might buckle during riveting risking not filling the hole properly or creating an asymmetrical shaped rivet head that will withstand lower axial forces than desired [Zarabi, R. (2005)].

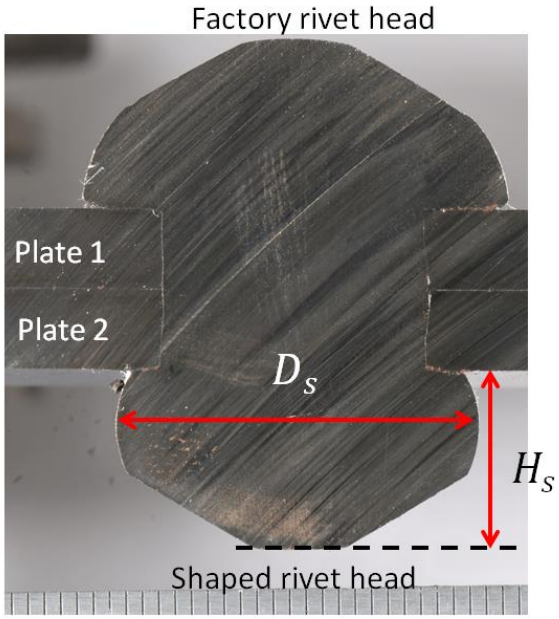

Figure 14 Cross section of riveted joint showing the shaped rivet head measurements.

2.2.9 Riveting force

Studies show that riveting force influences shaped rivet head diameter, filling of the hole and the squeeze stress of the joint. It is mentioned as an influential design parameter in several studies.

Jennfors, P. (1993) showed and later Abdulwahab, F. (2009) confirmed, that increased riveting force increased the fatigue life of a riveted joint, Figure 15. The studies focused on rivets with diameter between 15 mm and 18 mm. Baha II, S., Hesebeck, O. (2010), that investigated rivets with diameter 4 mm, also showed that riveting force is a major influence on the riveted joint.

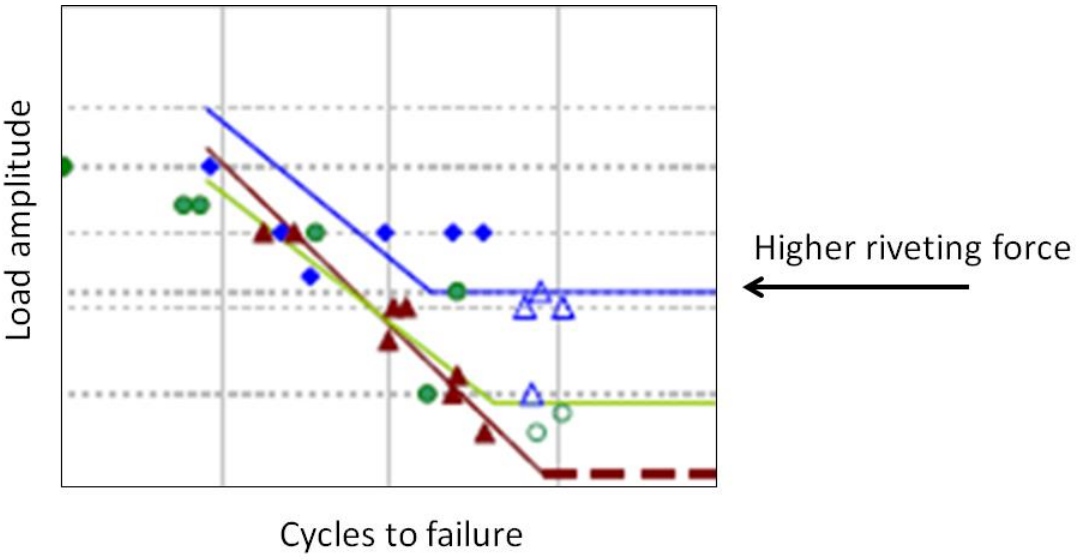

Figure 15 Higher riveting force increase the fatigue life [Abdulwahab, F. (2009)].

Fuiorea, I., Bartis, D., Nedelcu, R. (2009) showed that with a higher riveting force the load transfer by friction increased and the load transfer through the rivet shank decreased. The riveting force was also investigated by Skorupa, M., Skorupa, A., Machniewicz, T. et al. (2016), Skorupa, M., Skorupa, A., Machniewicz, T. et al. (2010) and Abdulwahab, F. (2009). They concluded that a higher squeeze stress increase the residual clamping between sheets which increase the load transfer by friction and therefore the fatigue life.

With a harder rivet the riveting force also needs to increase to reach the same amount of filling of the hole as a softer counterpart [Lacroix, D. (2016)]. Huan, H., Liu, M. (2017) studied the influence of riveting force for static loading and could there establish that increased riveting force was detrimental for the static strength of the riveted joint. That is expected as the rivet consist of a softer material than the plate and at static loading the rivet will fracture before the harder plates.

Important to note is that if too high riveting force is used undesired deformations in the plate can occur. The location of the crack initiation also moves away from the joint with higher riveting force and becomes increasingly difficult to predict due to the crack initiation can be triggered by harder granule in the material [Skorupa, M., Skorupa, A., Machniewicz, T. et al. (2010)].

2.2.10 Riveting speed

Abdulwahab, F. (2009) concluded that the speed of the riveting process influences the fatigue life as shown in Figure 16. With a rate dependent material the heat development during riveting influences material properties. Increased riveting force is needed at increased temperatures to reach the same strain level as for low temperatures. It is therefore important to consider the riveting speed in combination to the riveting force.

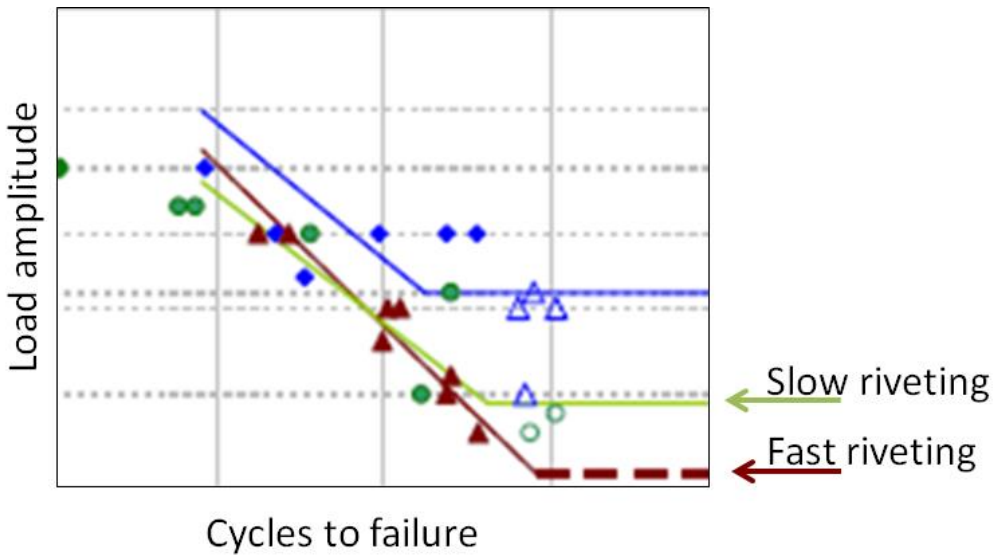

Figure 16 With a slower riveting speed the ultimate fatigue life is increased [Abdulwahab, F. (2009)].

2.3 Numerical simulation methods

Numerical simulations are often cost effective and relative quick compared to physical experiments [Ottosen, N., Petersson, H.(1992)]. A part of this study is to obtain a numerical simulation for evaluation of design parameters. It is therefore of interest to discover how other studies having performed numerical simulations of fatigue life estimations for the riveted joint.

Skorupa, M., Machniewicz, T, Skorupa, A. et al. (2015) discovered that the riveting process has to be considered to create good fatigue life estimation. The hole expansion and the load transfer path obtained during the riveting process is necessary to consider for a good fatigue life estimation. The load transfer path was closely related to the squeeze stress observed in the riveted joint. If only a geometrical representation of the riveted joints was used overestimation or underestimation of the fatigue life occurred. The numerical simulations conducted were verified to experimental data of shaped head diameter,D_s, and height, H_s as that were seen as the most important geometrical features.

Kaifu, Z., Hui, C., Yuan, L. (2011) used mathematics and FE- simulations to estimate the deformations of the plates and rivet during the riveting process. For the finite element (FE) - simulation they used ABAQUS software [ABAQUS (2017)]. A very fine mesh was used to capture the deformations during the riveting process, but no data of element size was stated.

Chen, N., Ducloux, R., Pecquet, C. et al. (2011) state that the performance of the riveted joint is influenced by many parameters, such as geometry, material and radial clearance. They built an FE model of the riveting process and validated that to experimental data to analyse and optimize the riveting process. Solid rivets in range between 5.8 mm $\leq$ D $\leq$ 14.9 mm were used. A half symmetric 3D FE- model was created in Forge2008 and Riv3D. They states that remeshing during the numerical simulation of the riveting process is almost always necessary to solve degeneration of element quality as very high strains are obtained during the riveting. Using remeshing techniques and a mesh size of 1 millimeter gave good geometrical accordance to their experimental data. The friction coefficient during the riveting process was chosen as 0.15 as they state that the friction coefficient has small impact on the final result of the riveting process. Validation of the FE- simulation was made to shaped head diameter,D_s, and height, H_s as since those were found to be the most important geometrical features for the strength of the joint.

Baha II, S., Hesebeck, O. (2010) created an FE- simulation and verified it to experimental data for evaluation of the friction coefficient between riveting tools and riveted joint. They used a 2D simulation using ABAQUS software with explicit time integration method. A desired element size of 0.05 mm for an $D = 4$ mm sized rivet was used. Arbitrary Lagrangian Eulerian (ALE) adaptive meshing was used to reduce the mesh distortion. The material model was described by isotropic elastic-plastic behavior. They stated that the only area where friction had a real influence during the riveting process was between the hammer die and shank. The friction influenced the geometry with a very limited influence on the residual stress fields. Their optimal friction coefficient was found to be 0.2.

Lipski, A. (2012) used ABAQUS software to analyze the effect of different hole treatments.

Skorupa, M., Skorupa, A., Machniewicz, T. et al. (2016) investigated how friction impacts fatigue life of riveted joints using numerical simulation together with fracture mechanics. They concluded that a pure FE modeling of fatigue life estimate of the riveted joint is not feasible due to changing friction at the plate interface during repetitive loading. a semi empirical approach is required to include the changing friction in the FE simulations.

Numerical evaluation of the riveted joint had only been performed in the studies published by the aviation industry. For numerical simulations to be performed for the vehicle industry other consideration may be needed than for the aviation industry.

To summarize, the following can be concluded from the literature study relevant to a numerical simulations that will be used to evaluate parameter influence of the riveted joint for the vehicle industry

- The riveting process is necessary to incorporate to create relevant fatigue life estimations. The simulation needs to capture the geometrical changes and the residual stress fields.
- For increased accuracy of fatigue life estimations the varying friction coefficient at the plate interface during repetitive loading needs to be incorporated.
- For aviation industry the hole penetration method was disregarded. But it may be necessary to include for the vehicle industry as different hole penetration methods can be used.
- The numerical simulation software used to simulate the riveting process in the majority of the studies was ABAQUS software. A very fine mesh or remeshing techniques were used to maintain the quality of the mesh. During the riveting process very high strains are created which can lead to sever distortions of the mesh. With severely distorted mesh, geometry and stress fields may not be accurately represented during the simulation.

2.4 Experimental methods

Experiments during this study will be conducted to validate the numerical simulation and to evaluate design parameters difficult to simulate. It was therefore of interest to investigate how other studies has conducted experiments for fatigue life estaimations.

Fatigue life experiments conducted previously at Volvo Group by, for example, Abdulwagab, F. (2010), Abdulwahab, F. (2009) and Jennfors, P. (1993) all used a single riveted lap joint and rivets with rounded heads. Experiments conducted for the aviation industry by, for example, Fuiorea, I., Bartis, D., Nedelcu, R. (2009) and Skorupa, M., Machniewicz, T, Skorupa, A. et al. (2015) used lap joints held together with several, smaller, rivets in thin plates. In aviation a wider range of rivet heads has also been investigated including round, flat and countersunk rivet heads. It was of primary interest to investigate how experiments had been conducted for larger rivets and thicker plates as this study focus on riveted joint dimensions for the vehicle industry.

The experiments performed by Abdulwahab, F. (2009), Abdulwahab, F. (2009) and Jennfors, P. (1993) used 7 mm plates and approximately 17 mm rivets. In their studies, experiments were conducted with unidirectional shear loading in hydraulic test rig machines. The loading was constant amplitude loading with ratio $R = -1$ to mimic the laod case of a truck. At least three different load levels were applied to represent possible load levels in a truck. The frequency of the applied load varied between $2 - 5$ Hz as the tensile test rig allowed. A Wöhler curve was created to compare different parameter influence of the fatigue life of the riveted joint.

To summarize, the following can be concluded from the literature study on experiments for cross members at Volvo Group

- Loading of a riveted joint in the truck can be represented by shear loading with load ratio of $R = -1$.
- Frequency of applied loading can be in the range $2 - 5$ Hz or as the loading rig allow.
- A Wöhler curve created by three load levels can be used to estimate the fatigue life.

2.5 Summary of the literature review

Three main features were identified during the literature review to influence the fatigue life of the riveted joint: filling of the hole, residual stress fields and load transfer path between plates.

During the literature review it could not always be determined if the design parameter identified had the same influence in vehicle industry as in aviation industry as different dimensions and materials are used. It is therefore stated after every design parameter in the following section if investigation has been conducted for the aviation industry (A) or the vehicle industry (V).

Filling of the hole was found to be one of the critical features for a strong joint, A fully expanded rivet is shown in Figure 17. The design parameters identified as influencing the filling of a hole was

- Rivet head design – A
- Hole geometry – V
- Riveting speed – V
- Rivet material – A & V
- Riveting force – A & V
- Radial clearance – A & V

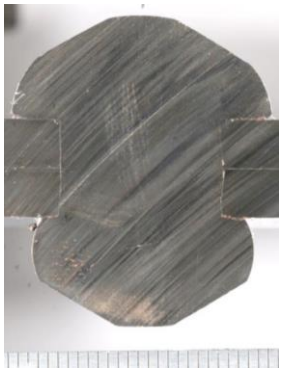

Figure 17 Cross section of a riveted joint.

Another important feature of the riveted joint is the residual stress fields. With smooth hole walls or compressive residual hoop stress, crack initiation was shown to be delayed in several studies. Skorupa, M., Skorupa, A., Machniewicz, T. et al. (2010) indicated that the squeeze stress, rather than shaped rivet head dimension, determine the fatigue strength of a riveted joint. Design parameters that was proven to have a major influence on the residual stress was

- Hole treatment – A
- Rivet and plate material – A & V
- Riveting force – A & V

The load transfer path was also found to influence the fatigue life. For high loads the fatigue life was increased with increased friction at the plate interface. For low loads reduced friction at the plate interface increased the fatigue life. Design parameters that was proven to have a major influence on the load transfer path was

- Plate material – A & V
- Surface treatment – A & V
- Riveting force – A & V

It was also identified that to obtain numerical simulation of a riveted joint that capture the fatigue life of the riveted joint three parts needs to be considered:

- Riveting process
- Hole penetration method
- Friction at plate interface

Several things needs to be considered to create a numerical simulation that is able to estimate the fatigue life of a riveted joint. The riveting process is critical to include as large residual stresses and deformations are obtained. Hole penetration method may be important, it depends on how large influence the method has on residual stress field, hole wall roughness and plate deformations. The changing friction at the plate interface, result of the produced fretting debris, increase in importance for increased number of load cycles.

3 Setup

In this section the investigated design parameters and the riveted joint setup is presented.

3.1 Design parameters to investigate

The primary design parameters that are investigated in this study are the hole geometry and hole treatment. Secondary design parameters investigated are plate material, rivet head design and plate edge cutting method. The choice of design parameters to investigate was inspired by the literature review. They were limited to what can be implemented with little effort in Volvo Group's current truck production and what available tools there were for the experiments.

During production of Volvo Group trucks stamping is mainly used to create the holes for the riveted joints, laser cutting is occasionally used for lower volume hole placements [Ragot, S (2018)]. Stamping and laser cutting produce different hole geometries and residual stress fields. As no previous studies had been found to investigate the hole geometry influence on filling, residual stress and therefore fatigue life it was chosen to investigate the hole geometry. As stamping tools were readily available for experimentation stamping was used as the hole penetration method.

Studies by Skorupa, M., Skorupa, A., Machniewicz, T. et al. (2016) and Skorupa, M., Skorupa, A., Machniewicz, T. et al. (2010) indicate that inducing compressive stresses in the hole walls dramatically increase the fatigue life. Therefore, different hole treatments was also chosen to be investigated.

Plate material was also considered as it, often, is a cost effective way of improving a design.

The plate cutting method was also investigated as it, possibly, can have effect on crack initiation and on the nominal mean stress of the joint.

The rivet head design is briefly investigated as one version exists for use during experiments (round head) and another version is easier to implement during numerical simulations (flat head).

All design parameters and the corresponding choices that are implemented in this study are presented in Table 1.

Table 1 Design parameters and the corresponding choices

Design parameters	Choices
Hole geometry	Convex hole geometry
	Hourglass hole geometry
	Stacked hole geometry with factory rivet head oriented at the narrow opening
Hole treatment	Pre punch
	Cold forming by mandrel
	Polishing by drilling a pre-stamped hole
Plate material	Material 1
	Material 2
Rivet head design	Round
	Flat
Rivet material	Material 4
Surface treatment	Non
Radial clearance	Nominally 0.5 mm [TR Rivet (2017)]
Hole penetration	Stamping
Shaped rivet head dimensions	As close to current truck production at Volvo Group as possible
Riveting force	RF, Current riveting force used in production of trucks at Volvo Group
Riveting speed	RS, available riveting tool speed during experiments

3.2 Riveted joint setup

A single riveted lap joint was studied, shown in Figure 18. The single riveted lap joint consists of two plates fastened together with a solid round headed rivet.

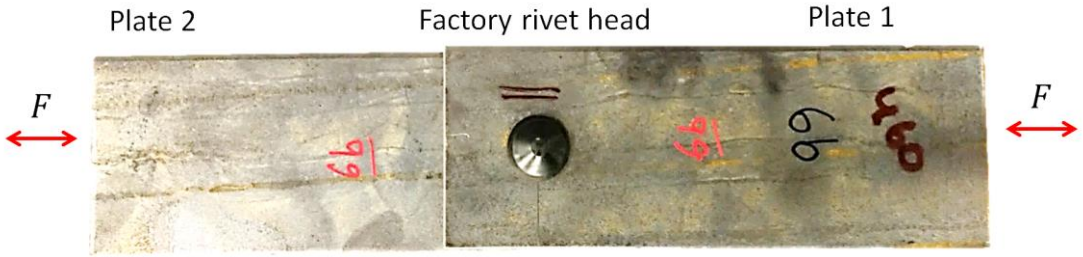

Figure 18 Typical riveted joint specimen, here TID 6b.

3.2.1 Rivets

The rivets for the frame sides in Volvo Group trucks have a nominal diameter of $D = 15$ mm and $D = 17$ mm when used in cross members [TR Rivet (2017)]. Round rivet heads are used in the frame sides and flat rivet heads in the cross members. The flat rivet heads are used when space is limited.

For experiments during this study round head rivets, $D = 15$ mm was available in varying length. The length of the riveted is determine by what amount of free length is

required to obtain sufficient filling and shaped rivet head diameter without the risk of buckling. For trucks at Volvo Group the free length is described in TR Rivet (2017). The needed rivet shank length for this riveted joint setup was 30 mm. The rivet standard material, Material 4, was used in the rivet.

3.2.2 Plates

The plate material that is investigated is Material 1 (the current cross member material) and Material 2 (the current frame side material). Higher strength steel, Material 3, was also considered but never investigated in this study due to time constraints. Material 3 was under production at SSAB at the time of the study and had a maximum thickness of $t = 5$ mm, it was used to determine the plate thickness for all plate materials. For the experiments, the plates were cut out of the sheets such that the loading was parallel to the sheet rolling direction. All materials were delivered without heat treatment by SSAB [Klintman, S. (2018)].

The dimensions of the rivets and the plates were estimated such that nominal stress and load transfer area in the riveted joint used in this study corresponds to similar nominal stress as in Jennfors, P. (1993). With similar nominal stress and load transfer area similar load levels can be used to represent the loading of a riveted joint in a cross member of a Volvo Group truck. For the plate in this study the only unknown parameter was then the width, w, of the plate. Width, w, plate length, L_{plate} , and hole placement are shown in Figure 19.

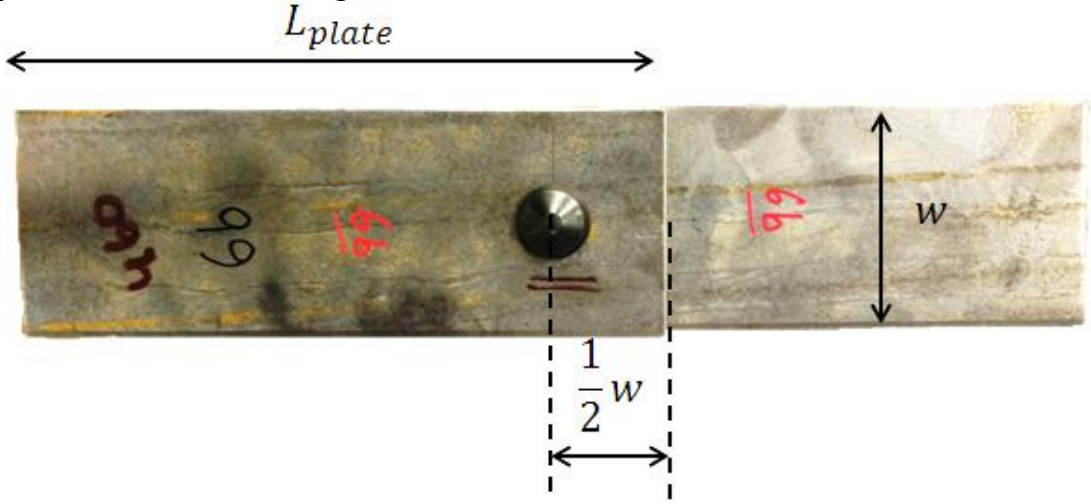

Figure 19 Dimensions of a test specimen

A cross sectional cut of the riveted joint gave the load bearing areas of rivet and plate as shown in Figure 20. The load bearing area of the rivet is simplified as a the cross sectional area A_{rivet}.

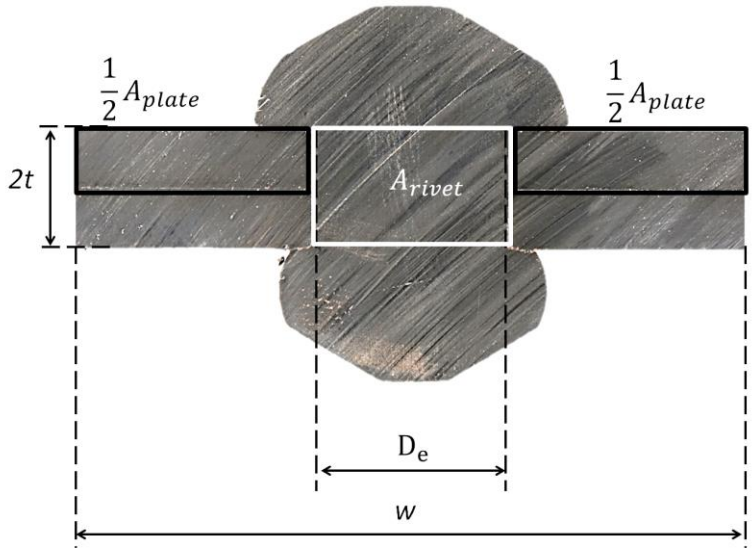

Figure 20 Dimensions of a riveted joint

The nominal shear force in the rivet is calculated as

$$\tau_{rivet} = \frac{F}{A_{rivet}} = \frac{F}{2t*D_e} \quad (3)$$

where F is the applied load as in Figure 18 and D_e the nominal width of the hole after riveting. The nominal stress in the plate is calculated as

$$\sigma_{plate} = \frac{F}{A_{plate}} = \frac{\mathrm{F}}{t*(w-D_e)} \quad (4)$$

were A_{plate} is the cross sectional area of the sheet on both side of the riveted joint. Using Equation (1) and (2) the ratio of stress transfer I by the rivet and by the plate is then calculated as

$$I = \frac{\sigma_{plate}}{\tau_{rivet}} = \frac{2\mathrm{D_e}}{\mathrm{w}-\mathrm{D_e}} \quad (5)$$

Using data from Jennfors, P. (1993) the ratio of desired stress transfer is then estimated as

$$I \approx I_J \quad (6)$$

The width, *w*, of the plate is then calculated by rewriting Equation (5) with known I from Equation (6) and using approximated dimensions for D_e

$$w = \frac{2D_e}{I} + D_e \approx 0.081 \text{ m} \quad (7)$$

The final dimensions used in this study are presented in Figure 21. The length of the plate is $L_{plate} = 230$ mm and is the same as for Jennfors, P. (1993) and Abdulwahab, F. (2009). The width of the plate is $w = 81$ mm as calculated in Equation (7). The nominal width of the hole, $D_h = 16$ mm as corresponding to hole dimensions used in

truck production at Volvo Group when using a rivet with diameter $D = 15$ mm. The hole is centered in the plate $\frac{1}{2}w = 40.5$ mm from the plate edge.

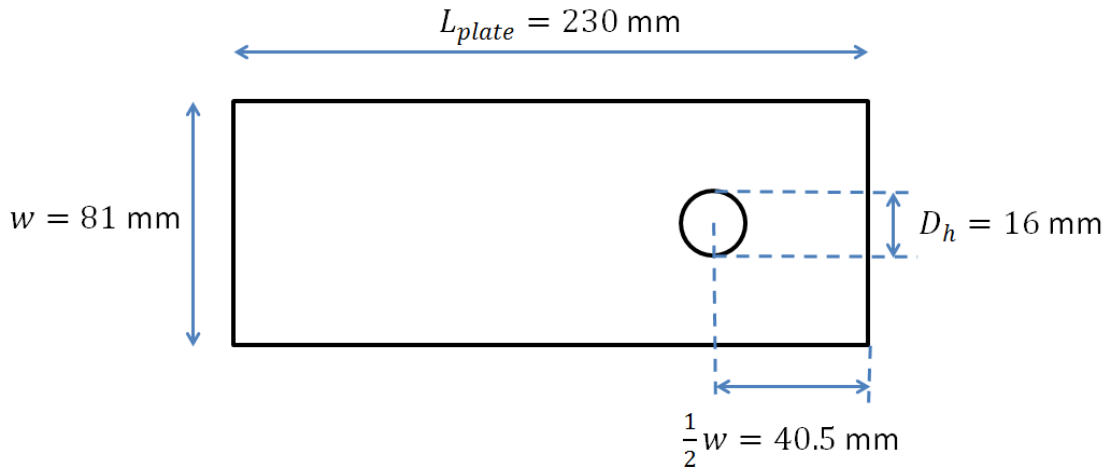

Figure 21 Plate dimensions

3.2.3 Assembly of the riveted joint

The plates was mechanically cut in rectangles of 230 x 81 mm. Mechanical cutting results in slight bending of the plates (increasing the residual nominal stress in the plate) and rough edges. Edge roughness is comparable to hole wall surface roughness obtained during stamping. Some plates were water cut. Water cutting only affects the nominal stresses a very small distance from the cut compared to the bending in the mechanical cutting produce. The edge produced during water cutting is also very smooth compared to mechanical cutting edge.

The hole was created by stamping with the center 40.5 mm from all plate edges. The stamping was performed using a punch with diameter corresponding to the desired hole diameter $D_{punch} = D_h = 16$ mm [TR Rivet (2017)]. The fixed die on the other side of the plate has a wider diameter than the punch, $D_{fixed} > D_{punch}$, to allow material to escape during the stamping process. For the plates used in this study the optimal clearance between punch and fixed die was 0.7 mm.

Riveting was conducted with riveting tools and riveting force, RF, corresponding to industrial truck production at Volvo Group [TR Rivet (2017)]. The riveting speed, RS, during the experiments was double compared to the industrial truck production at Volvo Group.

The riveting was conducted using squeezer ring to ensure full contact between plates. In production of trucks at Volvo Group bolts or other clamping rigs are used to hold plates together during the riveting process. The squeezer ring required two riveting steps. In the first step preliminary clamping of plates was accomplished, shown in Figure 22. The squeezer ring was placed around the free end of the rivet and then the rivet was compressed as much as the squeezer ring would allow. The squeezer ring was then removed.

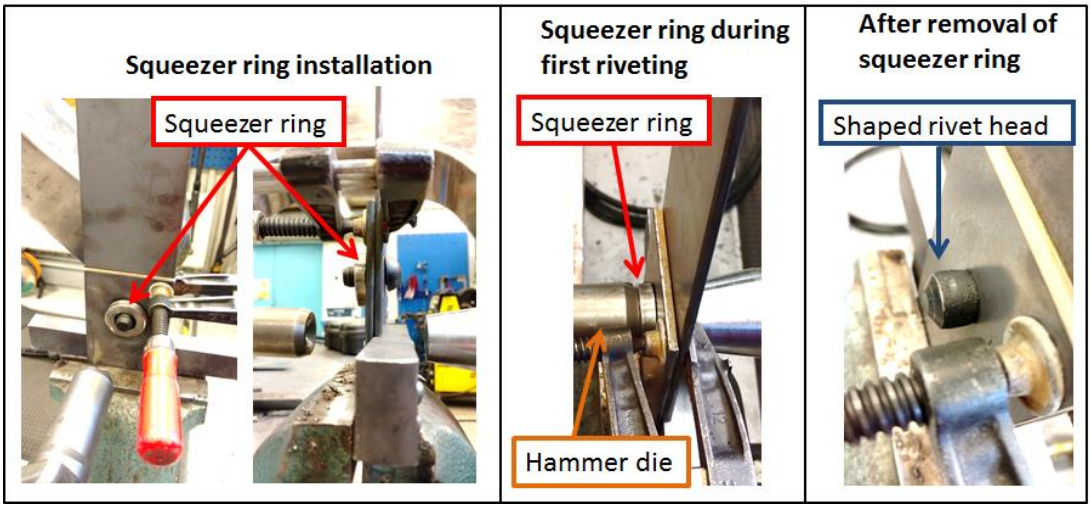

Figure 22 *Step 1: Create preliminary clamping with use of squeezer ring.*

In step 2 the final application of riveting force is applied creating the shaped rivet head. Figure 23 show the final shaped rivet head.

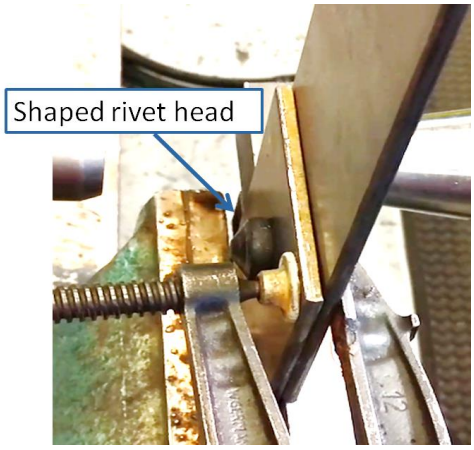

Figure 23 *Step 2: Final application of riveting force resulting in the shaped rivet head*

4 Experiments

Experiments were conducted for two reasons. The first reason was to verify the numerical simulation. The second reason was to evaluate design parameters that are difficult to evaluate numerically.

4.1 Hole wall geometry

This section evaluate how stamping affect the geometrical shape of the hole.

A nominal diameter of $D_h = 16$ mm was sought. Different fixed dies was therefore evaluated to identify the best tool dimensions. The hole dimensions investigated are shown in Figure 24. It can be observed that the right hand wall is straight while the left side wall is angled θ degrees. The unsymmetrical behaviour was due to a misalignment of punch and fixed die in the stamping machine. The straight hole edge was marked with two parallel lines on every test specimen to investigate the influence on fatigue life.

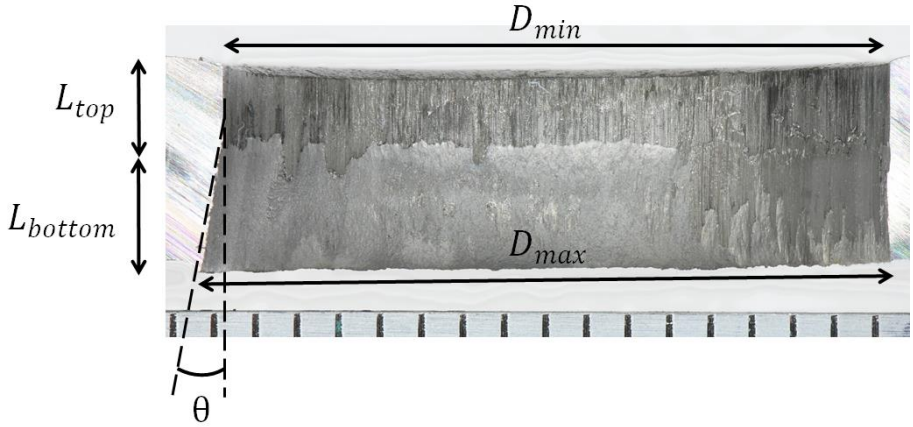

Figure 24 Hole wall dimensions for a stamped hole

Four different tool setups were investigated. The punch diameter, $D_{punch} = 16$ mm was held constant while the fixed die diameter was $D_{fixed} = 16.7$ mm and $D_{fixed} = 17.2$ mm. Two different materials, Material 1 and Material 2, were also investigated to study any potential differences in hole geometry due to material hardness. The different tool and material combinations are summarized in Table 2.

Table 2 Tests to evaluate hole geometry.

TID (Test ID)	**Name of test**	**Description**
1	Die16.7	$D_{fixed} = 16.7$ mm, Material 1
2	Die17.2	$D_{fixed} = 17.2$ mm, Material 1
3	Die16.7, Mat2	$D_{fixed} = 16.7$ mm, Material 2.
4	Die17.2, Mat2	$D_{fixed} = 17.2$ mm, Material 2.

The results of stamping as the hole penetration method is shown in Figure 25. The hole had wall diameters, D_{min} and D_{max}, that corresponded directly to the stamping tool diameters, D_{punch} and D_{fixed}. The left hand wall was consistently $L_{topp} = 2$ mm and $L_{bottom} = 3$ mm. No clear difference could be detected in the hole wall

roughness between Material 1 and Material 2. The asymmetry of the right and left hand side walls was about 10 degrees.

As $D_{fixed} = 16.7$ mm corresponded best to the dimensions used in production of Volvo Group trucks and was therefore chosen as the stamping tool.

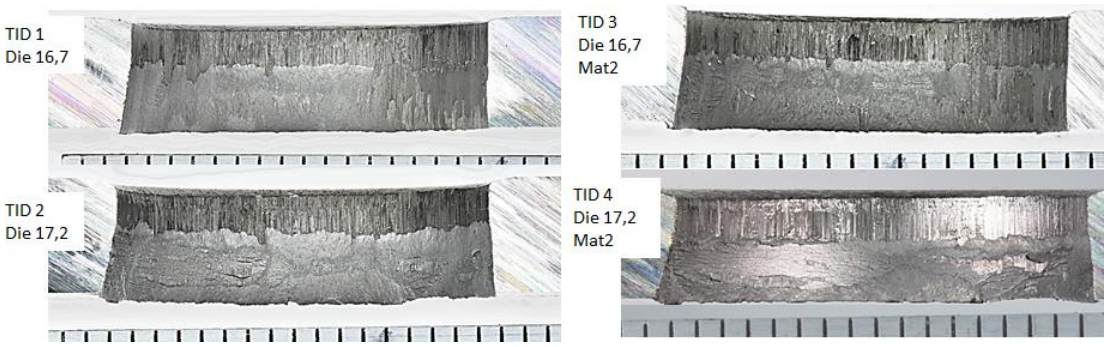

Figure 25 Hole wall geometry for different stamping tools.

4.2 Hole treatment

This section evaluate the geometrical effect of different hole treatments.

Four different hole treatment methods are evaluated: no treatment, pre punching, cold forming and drilling. The choice of hole treatment influences the initial stamping tool dimensions, summarized in Table 3.

Table 3 Tool dimensions for hole treatments

TID	Name of test	Description
1	Die 16,7	Step: Stamping, $D_{punch} = 16$ mm, $D_{fixed} = 16.7$ mm
13	Pre punch	1st step: Stamping, $D_{punch} = 15$ mm, $D_{fixed} = 15.7$ mm 2nd step: Stamping, $D_{punch} = 16$ mm, $D_{fixed} = 16.2$ mm
14	Cold forming by mandrel	1st step: Stamping, $D_{punch} = 15$ mm, $D_{fixed} = 15.7$ mm 2nd step: Cold forming by mandrel, $D_{mandrel} = 15.7$ mm
15	Drilling	1st step: Stamping, $D_{punch} = 14$ mm, $D_{fixed} = 14.7$ mm 2nd step: Drilling, $D_{drill} = 16$ mm

The results of the hole treatments are shown in Figure 26. Test ID (TID) 1 is the untreated hole while TID 13 – 15 are treated holes. All treated holes showed straighter and smoother walls than untreated wall in TID 1.

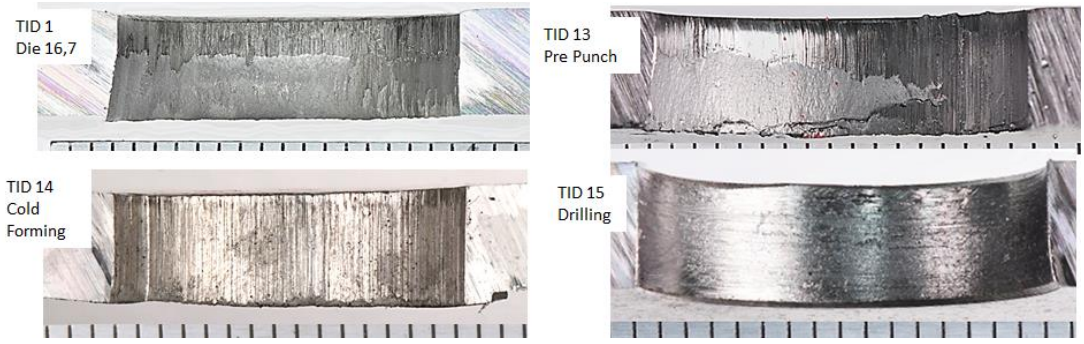

Figure 26 Hole wall geometry for different hole treatments

Pre punch treatment (TID 13) resulted in smoother and straighter walls than the untreated hole, TID 1. The clearance between punch and fixed die was 0.2 mm during the second stamping operation, compared to the 0.7 mm clearance between punch and fixed die used during the initial stamping.

Cold forming, using a lubricated mandrel, created straight walls with grooves in the axial direction. The lubrication was removed from the hole after treatments to avoid any influence on friction during fatigue life experiments. As the available mandrel had a diameter of $D_{mandrel} = 15.7$ mm the radial clearance between the rivet and hole wall was reduced to 0.35 mm from 0.7 mm.

Drilling created the smoothest walls of the different hole treatments. The edges of the hole were graded slightly to remove the burr left over from the drilling operation.

The differences in the hole walls are summarized in Table 4.

Table 4 Hole treatment results

TID	**Name**	**Nominal hole diameter, D_h**	**Surface**
1	Stamping	16.35 mm	Clear division between smoother and rougher wall. $\theta \approx 12°$
13	Pre Punch	16.1 mm	Smooth and rough patches. $\theta \approx 0°$
14	Cold forming by mandrel	15.7 mm	Groves in axial direction. $\theta = 0°$
15	Drilling	16 mm	Smoothest surface. $\theta = 0°$

4.3 Hole geometry

This section evaluate how different hole geometries influence the filling of the hole.

The hole filling was analyzed by studying the cross section of a riveted joint as shown in Figure 27**Error! Reference source not found.**.

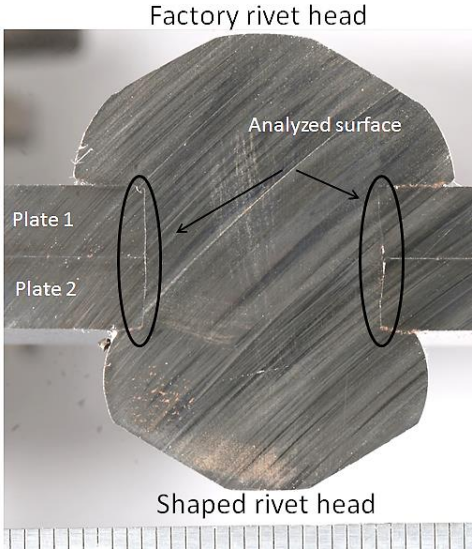

Figure 27 The analyzed surface for filling of the riveted hole

The different hole geometries investigated was: convex, hourglass and stacked narrow hole geometry, Figure 13, together with the treated hole geometries. Representative cross section cuts for the different samples are shown in Figure 28.

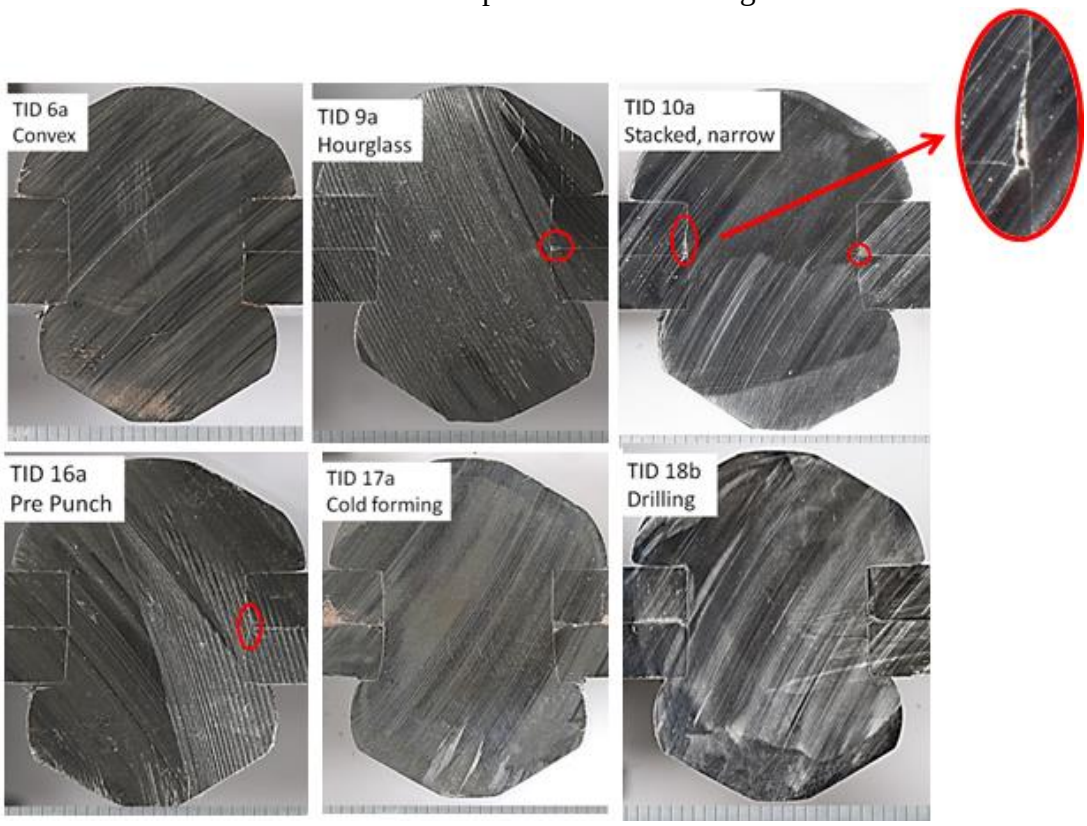

Figure 28 Representative cross sections showing the filling of the hole for different hole geometries. The larges void is showcased as well, 1.0 x 0.2mm.

When incomplete filling was observed, small voids existed between the rivet and the plate interface, as marked in Figure 28. The best filling was obtained with convex hole geometry using plate Material 1. With convex hole geometry and plate Material 2, a small void could be observed, possibly due to the hardness of the material. Both hourglass hole geometry and stacked narrow hole geometry shows developed voids, these hole geometries are from the beginning narrower around the middle which could explain the reduced filling. The result of Figure 28 is summarized in Table 5.

Table 5 Summarization of hole filling.

Filling	Description	Gap location	Gap size [mm]
No gaps	Convex, Material 1	N/A	
	Cold forming	N/A	
	Drilling	N/A	
Small gaps	Pre punch	Between rivet and plate 1	1.0 x 0.2
	Convex, Material 2	Between rivet and plate 2	1.0 x 0.2
	Hourglass	Plate interface	0.5 x 0.5
	Stacked Narrow	Between rivet and plate. Plate interface.	1.0 x 0.5 0.1 x 0.1

4.4 Shaped rivet head geometry

This section evaluates the shaped rivet head dimensions.

Dimensions of the shaped rivet head are shown in Figure 29. Maximum diameter of the rivet head is D_s , maximum height of the shaped rivet head is $H_{s,1}$ and $H_{s,2}$ indicates the edge height.

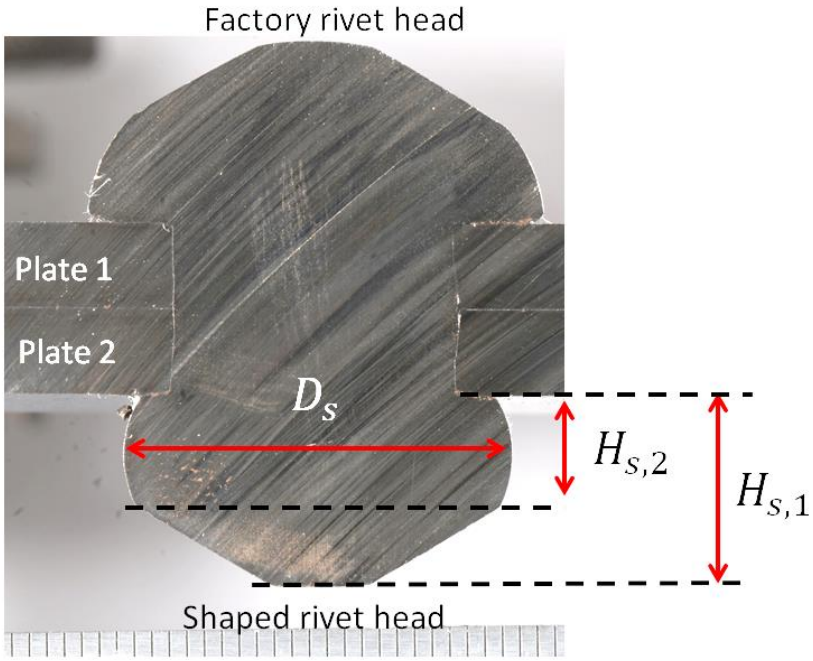

Figure 29 Shaped rivet head dimensions

The shaped rivet head dimensions were not affected by the differences in hole geometry. The average dimensions, based on 14 specimens, are shown in Table 6.

Table 6 Nominal shaped head dimensions, ± 0.1 mm

D_s	$H_{s,1}$	$H_{s,2}$
22 mm	11 mm	6.5 mm

The shaped rivet head height, $H_{s,1}$ was slightly larger, $H_{s,1}$ = 11.2 mm, with a decreased radial clearance. This was observed with the two cold forming treatments.

4.5 Heat dissipation

During the riveting process, the rivet plasticizes due to the applied riveting force. In other words, the material undergoes irreversible changes as the material is subjected to forces above its yield limit. Heat is generated during plactization due to friction in the material structure; slipping, twining and shear deformations occur as the material deforms. Additional, some heat will also be generated due to friction between parts. An attempt was made to measure the temperature increase during compression of a rivet.

A rivet, held in place by a thin plate, 0.5 mm, was placed between the hammer die and the fixed die in the riveting tool. A heat camera was used to record the surface temperature development during the compression.

The initial temperature of the rivet was $T^0 = 22.7$ ℃. Maximum temperature recorded was $= 88.3$ ℃ . The high temperature was measured in the rivet itself, indicating that the main heat contribution comes from the material plasticity.

4.6 Fatigue life experiments

This section evaluates the fatigue life experiments. A single riveted lap joint is subjected to shear unidirectional fatigue loading using a tensile test rig.

4.6.1 Tensile test rig setup

All fatigue life experiments were performed with a hydraulic tensile test rig with load cells of $S_{max,Rig}$ capacity. Figure 30 shows the tensile test rig with loaded test specimen. Plate distances of equal thickness to the test plates where placed within the hydraulic grips to mitigate bending.

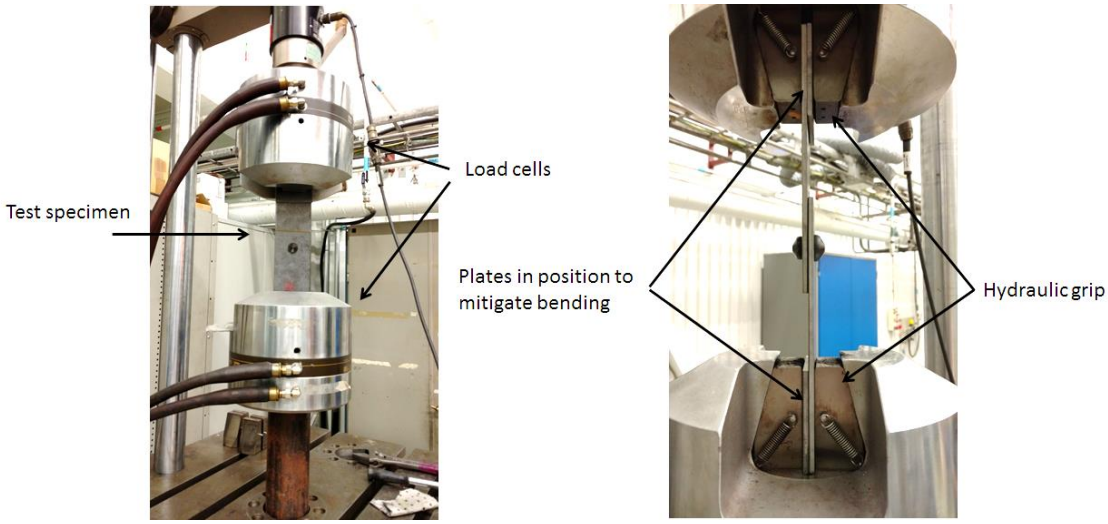

Figure 30 Tensile test rig.

One sample with convex geometry and no hole treatment (TID 6b) was subjected to a monotonically increasing load until $S_{max,Rig}$ had been reached, maximum of the tensile test rig. No cracks were observed in the joint. This indicates that this joint configuration can withstand static loading up to $S_{max,Rig}$ without failure.

4.6.2 Fatigue loading

Cyclic loading with constant amplitude was applied to the test specimen until fracture, Figure 31. The load ratio was $R = -1$. The loading is representative of a riveted joint in a cross member on a Volvo Group truck chassis [Abdulwagab, F. (2010)]. Three different load amplitudes are applied: low amplitude of $S_{max,L}$, medium amplitude of $S_{max,M}$ and high amplitude of $S_{max,H}$. The loading frequency was $f = 5$ Hz, higher frequency resulted in severe vibration of the rig and overshooting of the actual applied load compared to the desired.

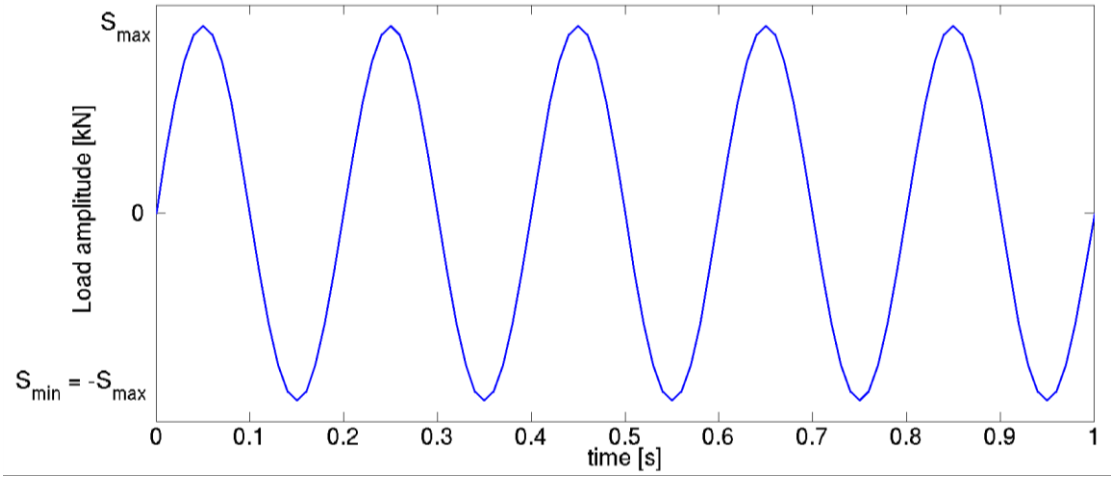

Figure 31 Fatigue load.

The loading was stopped when the critical displacement, $disp_{crit}$, of the hudrailic grips had been reached, Figure 32. The critical displacement was chosen to allow a crack to form but not to allow too many additional load cycles to run. The desire was to keep the evidence of the crack nucleation site for optical analysis. The initial displacement of the hydraulic grips were $disp_{init} = 210$ mm and the critical

displacement were reached at $disp_{crit} \geq 0.6$ mm. For higher load amplitudes the critical displacement was increased to $disp_{crit} \geq 0.8$ mm to allow for the larger displacements that occurred with the higher S_{max}.

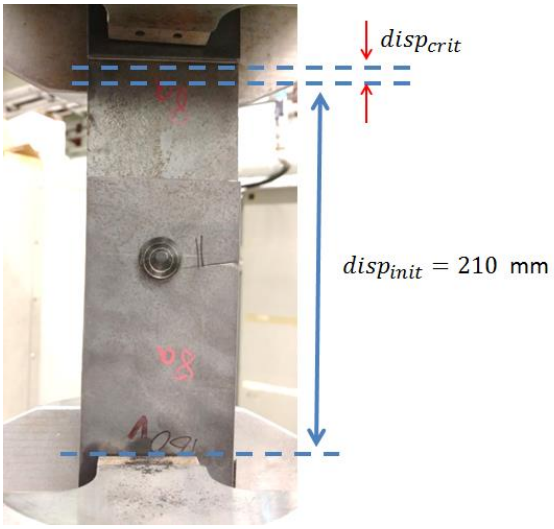

Figure 32 Critical displacement of the hydraulic grips.

4.6.3 Load cycles to failure

The hole geometry were evaluated at high load ($S_{max,H}$) and low load ($S_{max,L}$). Hole treatments were evaluated at medium load ($S_{max,M}$). The different investigated specimens with respective load level are summarized in Table 7.

Table 7 Specimens subjected to fatigue loading

TID	Name	S_{max}	Description
7	Convex	$S_{max,L}$, $S_{max,M}$, $S_{max,M}$, $S_{max,H}$	Convex hole geometry
8	Convex, water cut plate	$S_{max,L}$, $S_{max,H}$	Convex hole geometry with water cut plate boundaries
9	Hourglass	$S_{max,L}$, $S_{max,H}$	Hourglass hole geometry
10	Stacked narrow	$S_{max,L}$, $S_{max,H}$	Stacked hole geometry with factory rivet head at narrow opening
11	Convex, Mat2	$S_{max,L}$	Convex hole geometry with plate material as Material 2
16	Pre punch	$S_{max,M}$, $S_{max,M}$	Treatment: stamping $D_{punch} = 16$ mm, $D_{fixed} = 16.2$ mm
17	Cold forming	$S_{max,M}$, $S_{max,M}$	Treatment: Cold forming by mandrel, $D_{mandrel} = 15.7$ mm
18	Drilling	$S_{max,M}$, $S_{max,M}$	Treatment: Drilling, $D_{drill} = 16$ mm

The fatigue life results, load cycles to failure (N), are presented in Figure 33. Few samples were tested. The results have low statistic certainty. The normal distribution of riveted joints normally vary by a factor of 4 to 5 [Ragot, S (2018)], which cover the hole distribution range at $S_{max,L}$. But even with the low statistic certainty an indications of trends can still be estimated.

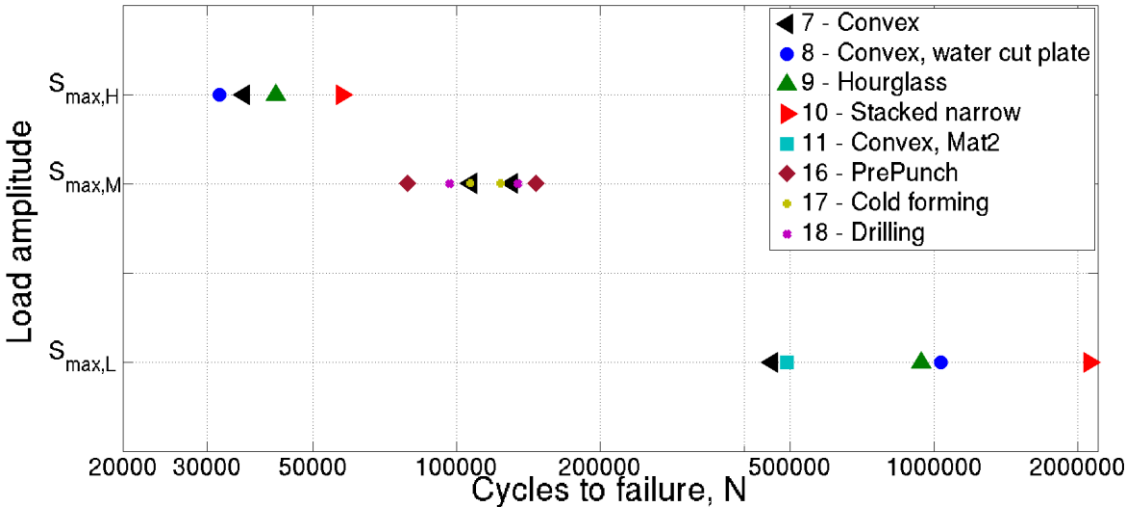

Figure 33 Load cycles to failure

Hole geometry (TID 7 – TID 11)
A larger scatter at $S_{max,L}$ than at $S_{max,H}$ is identified. Indicating that hole geometry may have a larger influence at low loads.

The stacked narrow hole geometry (TID 10) performed best at both load levels, indicating that this may be a superior configuration.

No detrimental effect could be observed between fatigue life and occurrences of the small voids due to incomplete filling.

Plate Material (TID 7, TID 11)
Material 1 (TID 7) is compared to Material 2 (TID 11) for convex hole geometry at $S_{max,L}$. Very similar fatigue life is observed, but as only one sample with Material 2 was tested no conclusions can be drawn.

Nominal stress in plates (TID 7, TID 8 and TID 11)
The specimen with water cut plate boundaries (TID 8) performed better than the specimens with mechanically cut plate boundaries (TID 7, 11) at $S_{max,L}$. This indicates that the riveted joints fatigue life may be influenced by the higher nominal stress in the plate that was obtained due to the slight bending of the mechanically cut plates. No cracks initiated at the plate edges, indicating that the surface roughness at the plate edges do not influence crack initiation when the hole wall is located 32 mm from the plate edge.

Hole treatment (TID 7, TID 16 – TID 18)
No definitive results regarding best fatigue life, due to hole treatment, can be observed at $S_{max,M}$. Deviation between samples can indicate reliability and repeatability of the different hole treatment methods. Cold forming with mandrel (TID 17) and no treatment (TID 7) gave the smallest deviation between samples, indicating high repeatability and good consistent quality of the joint. The largest deviation between samples where observed for pre punch (TID 16), indicating a less optimal joint configuration. The critical displacement, $disp_{crit}$, was by mistake set to an order of two larger for one of the drilled samples (TID 18a), making the comparison of deviation between the two drilled samples (TID 18) inconclusive. But even with

the larger critical displacement the drilling produced smaller deviation between samples than pre punching, indicating a better joint configuration.

All conclusions drawn from fatigue life evaluation of Figure 33 are summarized in Table 8.

Table 8 Indicated fatigue life of design parameters

Low load	**Best hole geometry**
	Stacked Narrow
	Hourglass
	Convex
	Best plate cutting edge method
	Water cut
	Mechanically cut
Medium load	**Most consistent hole treatment**
	Cold forming
	No treatment
	Drilling (inconclusive)
	Pre Punch
High load	**Best hole geometry**
	Stacked Narrow
	Hourglass
	Convex

4.6.4 Failure modes

Different load levels resulted in different failure modes. The rivet shank fractured at high loads. The plates fractured at low loads. Small cracks in plate and rivet occurred at medium loads.

High load
All specimens fractured in the rivet shank for $S_{max,H}$. The fractures were initiated at the plate interface as shown in Figure 34. The rivet material (Material 4) is a softer and more ductile material than the plate materials (Material 1 and Material 2) and at high loads the rivet will always fracture before the plate. There was no indication that the hole geometry influenced the failure mode.

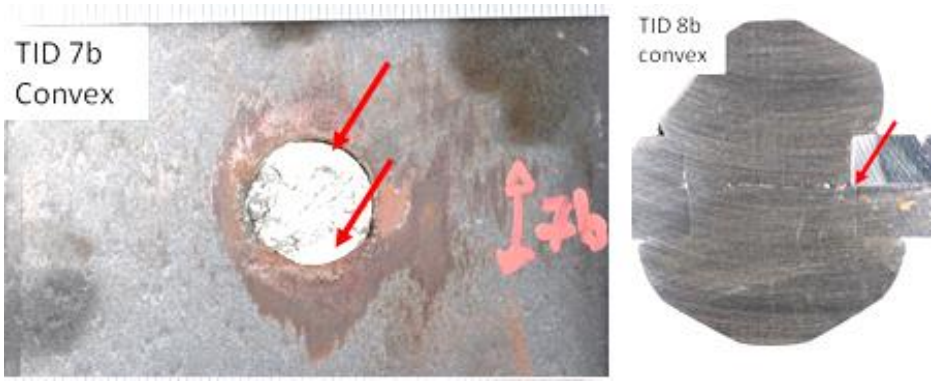

Figure 34 Crack initiation site indicated by arrows, $S_{max,H}$.

Medium load

All specimens fractured in the plate for $S_{max,M}$. Several small cracks were observed initiated around the hole with one crack propagating further, leading to failure. That several cracks had been initiated indicates that the plate material had simply reached a critical load level. The different hole treatments led to slightly different crack initiation sites.

With no treatment of the hole (TID 7) and hole treated by pre punched (TID 16) similar crack initiation and propagation of the cracks were observed, Figure 35. The largest crack that lead to failure occurred in plate 2.

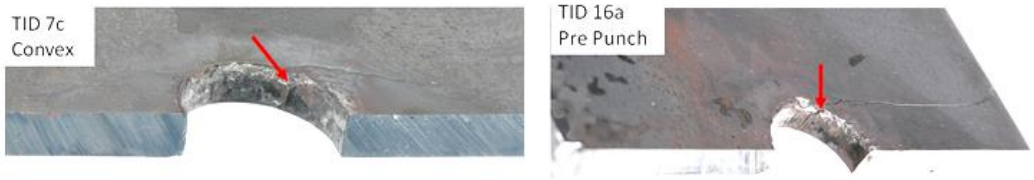

Figure 35 Largest crack initiation site indicated by arrows. Load $S_{max,M}$ for specimens with no hole treatment and hole treatment by pre punch.

Several fine cracks were observed in plate 1, plate 2 and in the shank for the hole treated with drilling (TID 18),
Figure 36. The many small evenly propagated cracks indicates that the loading was evenly distributed and no clear stress concentration points existed.

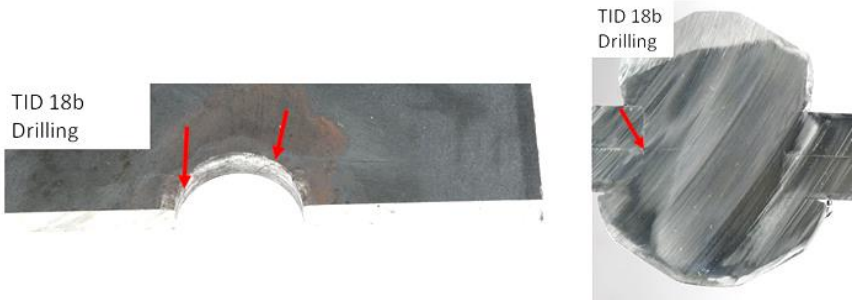

Figure 36 Crack initiation site indicated by arrows. Load $S_{max,M}$ for specimens with hole treated by drilling.

The hole treated with cold forming with mandrel (TID 17) cracked 4 mm from the hole edge, Figure 37. The crack initiated at the plate interface in plate 1. The crack

initiations site indicates that the compressive stresses in the hole walls do influence the response of the riveted joint.

Figure 37 Crack nucleation indicated by arrows. Load $S_{max,M}$ for specimens with hole treated by cold forming.

Low load

Only one main, well developed, crack could be observed for $S_{max,L}$, Figure 38. This indicates that the crack initiation occurred at a stress concentration point. The fretting area around the hole was also larger than for the higher load cases, indicating a possible larger change in friction at the plate interface. The cracks propagated into plate 1 or in plate 2 at this load level.

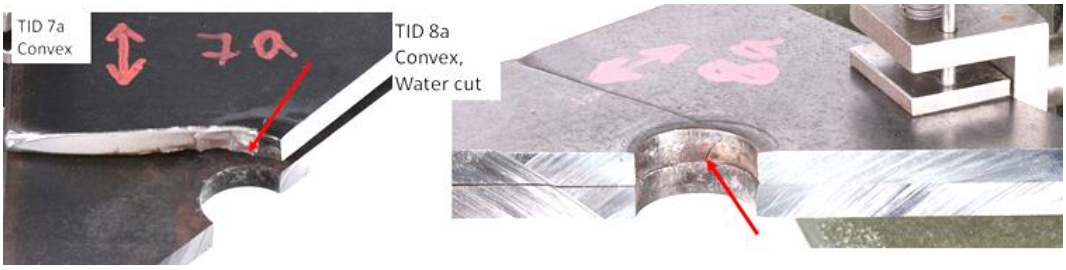

Figure 38 Crack initiation site indicated by arrows. Load $S_{max,L}$ for convex hole geometry.

For stacked narrow hole geometry (TID 10) no fracture could be observed. The experiment was terminated at 2 million cycles when no indication of fracture occurred.

4.6.5 Failure location

Crack initiations occurred at 45 degree to the loading direction for $S_{max,L}$ and $S_{max,M}$ as shown in Figure 39. The two parallel lines at 90 degree to loading direction indicate the location of the straight hole wall section that was the result of the not completely centered stamping tools.

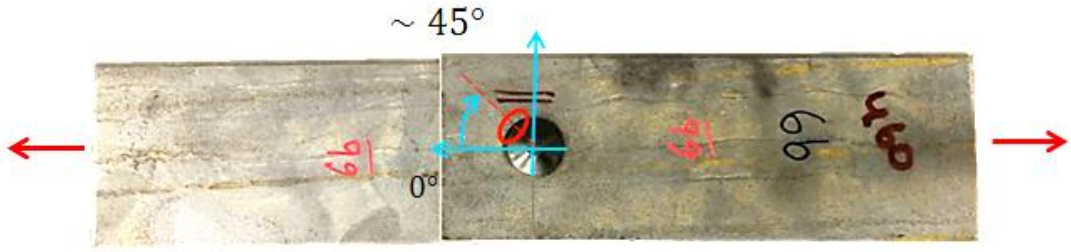

Figure 39 Crack initiation for $S_{max,L}$ and $S_{max,M}$.

Crack initiations for high loads, $S_{max,H}$, occurred between 0 – 110 degrees to the loading direction as shown in Figure 40. The exact crack initiation location could not be determined.

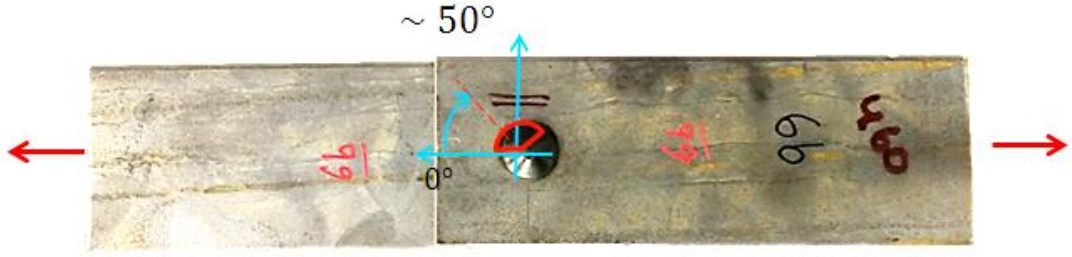

Figure 40 Crack initiation for $S_{max,H}$.

All cracks initiated in or around the plate interface close to the hole wall, position A to E in Figure 41. For high loads the crack initiation locations occurred in the rivet shank at the plate interface, location A. For medium loads the crack initiation locations occurred in the hole wall at the plate interface at position A, B or D. Crack initiation locations away from the hole wall, at position D, occurred only for cold forming by the mandrel. For low loads the cracks occurred mainly in plate 2 initiated in the hole wall at the plate interface, location D. With the exception of on specimen fracturing in plate 1, location B, and one crack initiation not in the hole wall, location E.

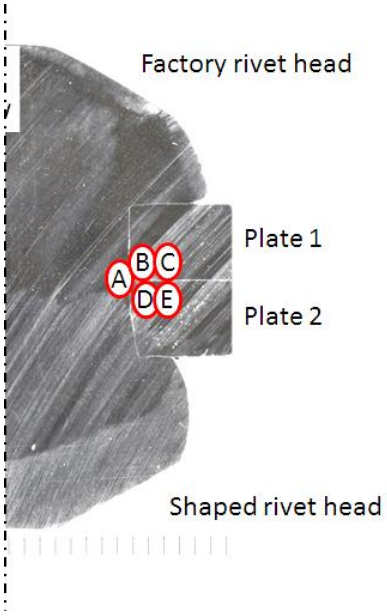

Figure 41 Crack initiations

4.6.6 Fretting

Fretting occurred between all contact surfaces during the fatigue loading of the riveted joint.

The fretting at the plate interface was examined. It was clear that the affected area around the hole increased with number of load cycles, as expected. From $S_{max,H}$ to $S_{max,L}$ the area increased approximately 2 mm in radial direction for all samples, Figure 42.

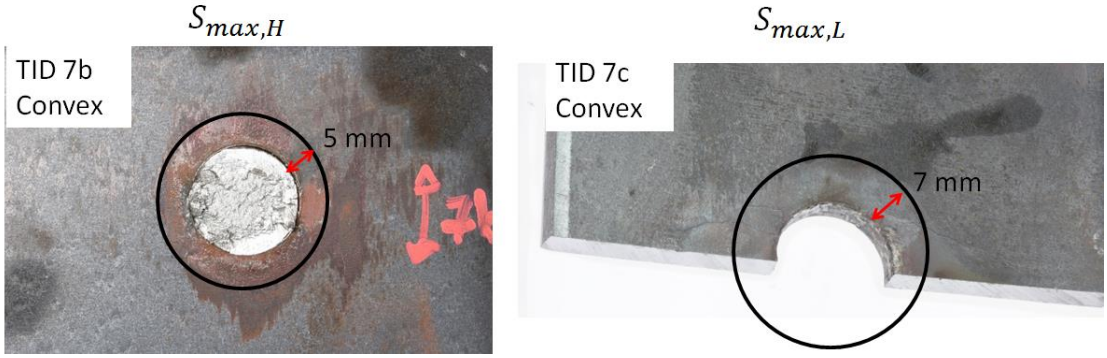

Figure 42 Fretting area for high and low load at plate interface.

The rivet also experienced fretting with the largest affected area in the rivet shank, as shown in Figure 43. The uneven fretting indicate difference in contact pressure with the higher shine, marked area in Figure 43, corresponding to reduced contact pressure between rivet and plates.

Figure 43 Fretting of rivet shank

4.7 Error sources

This section describes the possible sources of error for the experiments conducted during this study.

One source of error was the unsymmetrical hole wall geometry due to the non-calibrated stamping tool. All fractures during the fatigue life experiments occurred at the straighter hole wall. This indicates that the hole geometry do influence fatigue life and that the a straighter hole wall is the limiting hole geometry. It is possible that no other hole geometry really has been investigated in this study except the straight hole wall geometry.

Another source of error was the uncertainties during assembly of the test pieces as no assembly rigs were used. Hole treatments were guided by hand and may have influenced the symmetry response of the hole. The riveting tools were also guided by hand, and may have been a contributing factor to the slight unsymmetrical rivet head geometry. It is unknown how much the asymmetry impacted the fatigue life.

The full temperature increase in the rivet during the riveting process may not have been fully measured. There was no available rig that could hold the rivet steady to avoid the half compressed rivet slipping out of the riveting tool without simultaneously concealing the rivet from the heat camera. This may have resulted in measurement errors.

The placement of the tensile test rigs hydraulic grips on the specimens induced bending in the riveted joint and may have affected the fatigue life.

Statistic confidence for the fatigue life evaluation is limited due the too few test samples. No normal distribution can be assumed. Results in this study may be typical or atypical, without further samples that cannot be determined.

The fatigue life assessments may be conservative as the critical displacement was set to interrupt the loading cycles before complete failure had occurred. It was judged that finding the exact crack initiation was more relevant than identifying the exact number of load cycles to failure.

Errors in crack evaluation and hole filling evaluation may have been induced. After the fatigue life experiments the specimens were cut in two halves. The half of the riveted joint exhibiting the main crack was thoroughly investigated for cracks and fretting. The other half was used to determine hole filling and shaped rivet head dimensions. It is possible that data may have been concealed when evaluation of each feature only occurred for half of the test specimen.

It is also possible that measurement errors of hole wall dimensions and shaped rivet head dimensions occurred. No rig was used when the test specimens were halved to ensure that the cut was made exactly at the center of the riveted joint. The possible off centered cross section cut may have resulted in measurement errors.

4.8 Summary of the experiments

This section summarizes the experimental results.

Straight hole walls was found to be the limiting hole wall geometry. The stacked narrow hole geometry was indicated as the best hole geometry. No indications of best hole geometry could be identified between convex and hourglass hole geometry.

Hole treatments produced straighter hole walls with reduced wall roughness. Cold forming by mandrel was indicated as a good hole treatment when consistent results are desired, closely followed by no hole treatment. Even load distribution in the riveted joint was found for the hole treated with drilling. Hole treated with pre punch was identified as the least beneficial hole treatment.

The failure mode was load dependent. The rivet sheared for high loads as the softer rivet material failed before the harder plate material. Several fractures developed in the plates for medium loading as the plate completely failed. A fatigue induced crack was created for low loads where one crack lead to failure.

For all test specimens the crack initiation occurred 45 degrees to loading direction at the plate interface.

It is indicated that water cutting the plate edges improved the fatigue life. With the water cut plate edges the nominal residual stress in the plate is reduced as no bending occur, compared to using mechanical cutting. The roughness of the plate edge cut did not influence crack initiation as all cracks initiated in and around the hole walls.

No distinct difference in hole wall geometry or hole wall roughness could be observed between plate Material 1 and plate Material 2. Due to the limited number of test specimens during experiments no fatigue life comparison between Material 1 and Material 2 could be made.

The temperature during compression of the rivet reaches at least $T = 88.3$ ℃ in room temperature.

The larger fretting area at the plate interface around the riveted joint for low loads indicates a larger change of friction coefficient for lower loads and therefore a change of load transfer path.

Small voids, 1.0 mm x 0.5 mm, between rivet and plate interface could not be observed as having a detrimental effect on fatigue life.

At least $S_{max,Rig}$ tensile shear load could be applied to a riveted joint with convex hole geometry without fracture

5 Numerical simulations

Two numerical simulations will be described in this section. The first simulation is of the riveting process. The numerical riveting simulation can be used to evaluate filling of the hole and residual stress fields of different design parameters. The simulation can in future studies be expanded to include simulation of penetration operation to further consider geometrical and residual stress field influence on different design parameters. Material data for fatigue and fracture can also be incorporated in the simulations to allow for numerical fatigue life evaluation. The second simulation evaluates the stress fields that occur due to shear loading of a riveted joint. The FE-model consists of a simplified riveted joint were residual stress fields and geometrical changes from the riveting process are disregarded.

The preprocessor ANSA version 18.0.1 [ANSA (2018)] was used to create the FE-models as it was readily available at Volvo GTT. The FE software ABAQUS was then used for the numerical simulations. At Volvo GTT the version ABAQUS 3DEXPERIENCE R2017X [ABAQUS (2017)] was available and therefore used during this study.

5.1 Riveting process simulation

This section describes the numerical riveting process simulation. The goal was to be able to use the simulation to evaluate design parameters effect on geometry and residual stress fields.

5.1.1 FE -model

A quarter of the riveted joint was modeled in ANSA (using symmetry conditions) to decrease simulation time, Figure 44. The FE-model consisted of the rivet, two plates and the riveting tools fixed die and a hammer die.

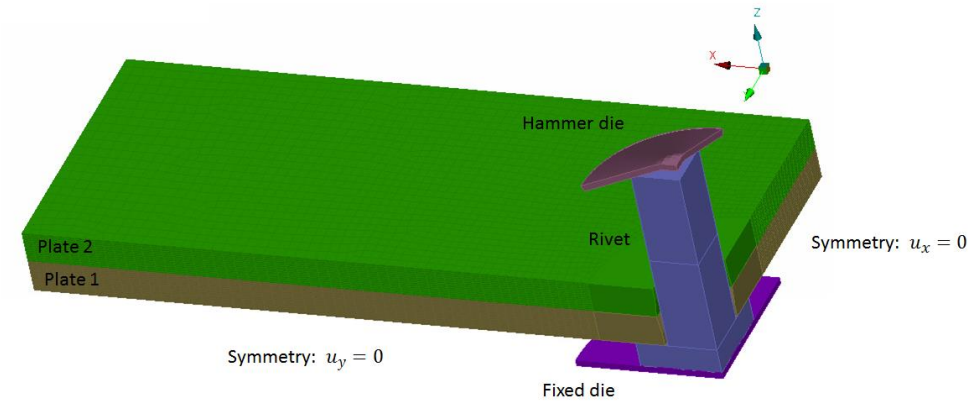

Figure 44 Quarter symmetrical FE- model of riveted joint.

The quarter FE-model could easily be expanded if desired in the future. A half symmetric FE- model would be recommended for application of shear loading to allow bending effects in the joint. A full model would be recommended when performing evaluation of unsymmetrical behavior due to different design parameters.

The rivet geometry was simplified, no rounded edges and only small chamfers. The rivet diameter was chosen as $D = 15$ mm, corresponding to experimental data. The factory rivet head was kept flat to simplify meshing operations. The full plate length

was not included in the FE-model. The plate area where the hydraulic grips of the tensile test rig were holding on to the specimens was disregarded. The final plate dimensions are shown in Figure 45 together with the rivet diameter.

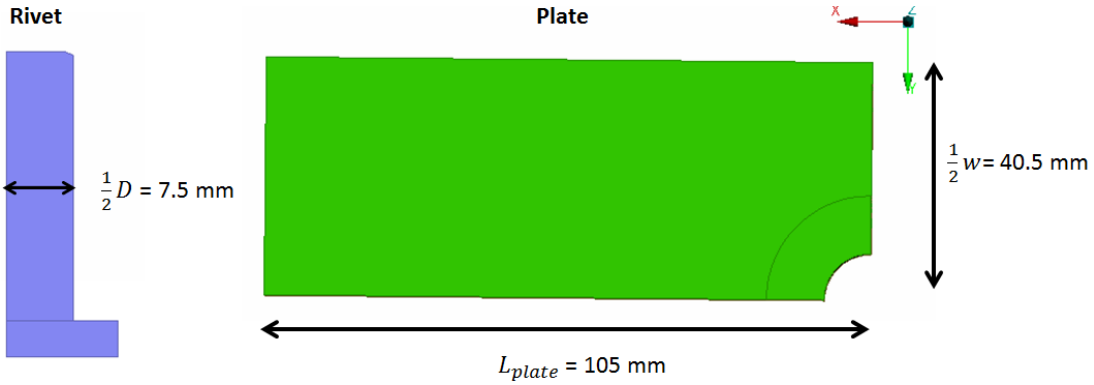

Figure 45 Simplified rivet geometry and plate dimensions for.

The main hole penetration method during truck production for Volvo Group is stamping. The stamping was simulated as a geometrical feature only in the FE-model, shown in Figure 46. The residual stress fields from the stamping operation is assumed to be less than what is obtained during the riveting process, and therefore disregarded. Hole wall roughness is also disregarded as it would require additional experimental data.

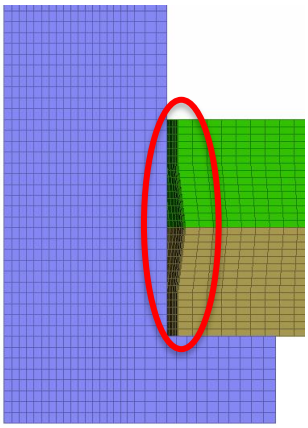

Figure 46 Hole wall shaped due to stamping. Convex hole geometry.

The riveting tools, hammer die and fixed die, were represented by rigid elements to prevent deformations of the dies and reduce computational time.

5.1.2 Material model

Plate and rivet material models were defined from experimental data. Elastic strain, ε_e, and plastic strain, ε_p, were needed for the simulations models.

Plate material data were extracted from tensile tests conducted at Volvo Group. The tensile tests included the stress, σ, and strain, ε, response. The plastic strain, ε_p, and elastic strain, ε_e, were estimated as

$$\varepsilon_e = \frac{\sigma}{E} \quad (9)$$

$$\varepsilon_p = \varepsilon - \varepsilon_e \quad (10)$$

with Young's modulus, E, estimated from the elastic strain range.

$$E = \frac{\sigma}{\varepsilon} \quad (11)$$

Rivet material data were estimated from experimental yield strength, σ_y, and ultimate tensile strength, σ_u.

All material models were assumed isotropic. The materials for the different parts of the FE-model are shown in Table 9.

Table 9 Material data in FE-model

Part	**Material**
Plate 1	Material 1
Plate 2	Material 1
Rivet	Material 4
Hammer and fixed die	Rigid body elements

ABAQUS parameter NLGEOM is activated to account for large deformations and nonlinear geometrical responses [ABAQUS guide (2014)].

5.1.3 Mesh size and element shape

A finer mesh was used in and around the riveted joint to capture residual stress fields and deformations. The element length aimed for was 0.5 mm, Figure 47.

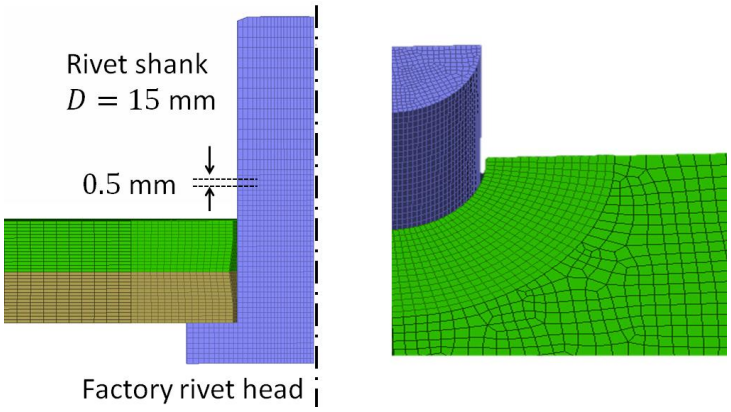

Figure 47 Mesh in and around the riveted joint.

The elements in the top of the rivet shank are rectangular to allow for the severe axial compression during the riveting, Figure 48. The element size is 0.5 x 1.0 mm.

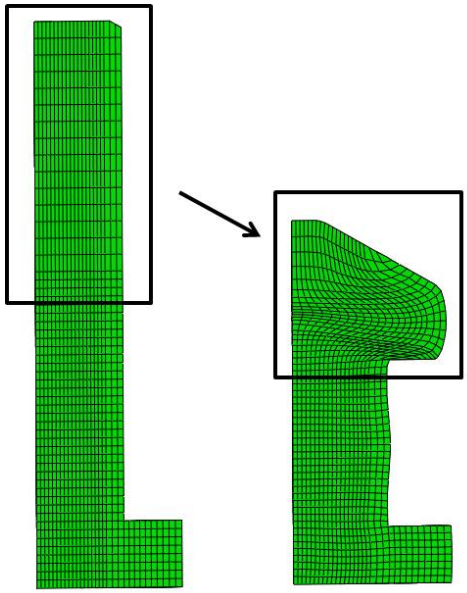

Figure 48 Undeformed and deformed rivet shank mesh.

The element shape was chosen as a brick type element to simplify the almost uniaxial compression of the elements in the rivet shank. The standard brick elements of type C3D8R were used. It is a 3D solid element with hourglass control. Additionally, the C3D8R element is an element that can be used together with adaptive meshing methods in ABAQUS [ABAQUS guide (2014)] if improved mesh quality is needed in the rivet shank.

5.1.4 Boundary conditions

The two symmetry planes were fixed in x- and y-direction for the quarter riveted joint FE-model. The fixed die was additionally restricted also in the z- direction. The hammer die only had z-direction free for the application of riveting force. The boundary conditions are shown in Figure 49.

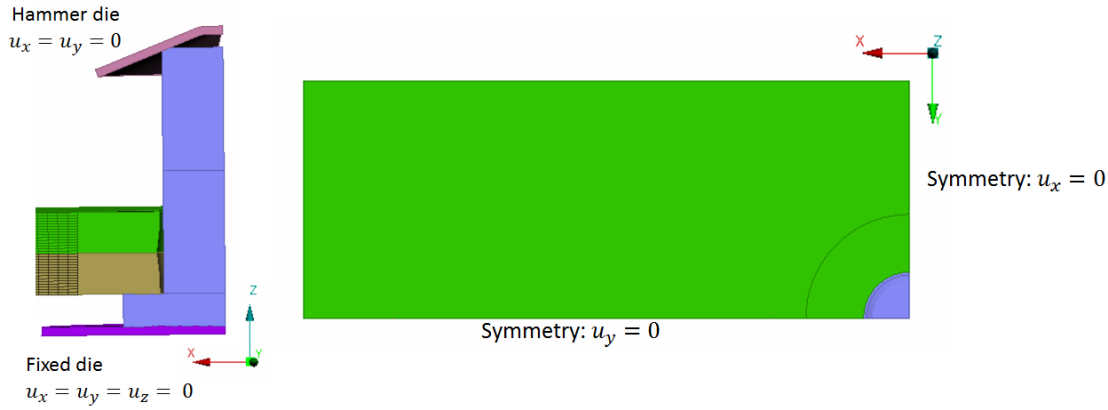

Figure 49 Boundary conditions for riveting tools and symmetrical boundary conditions for FE-model.

Different ways to prevent relative movements of the plates were investigated, Figure 50. Small plates were simulated by having no boundary conditions placed on the plate edges. Simulating that the riveted joint is part of a larger structure was made by fixing the plate edges in space. A squeezer ring was simulated by tying part of the plate interface together. Further investigations are needed to properly determine what plate

restriction best correspond to experimental data. Without the further experimental data fixed plate edges are assumed to best represent the riveted joint during industrial production, it is therefore used.

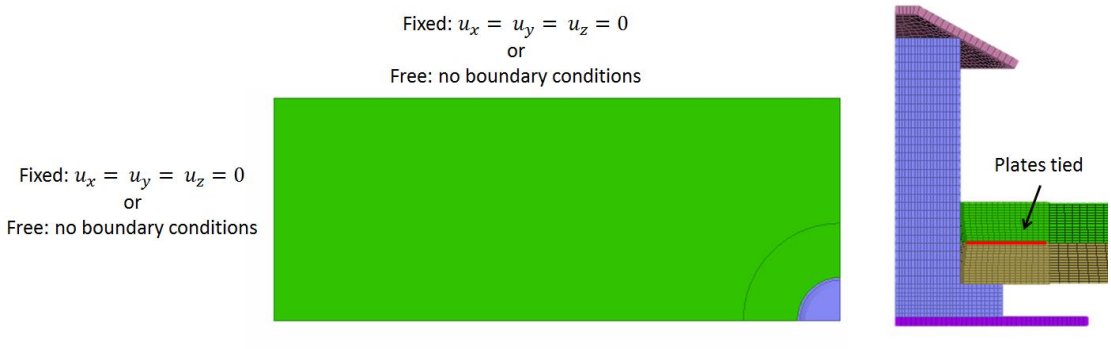

Figure 50 Boundary conditions to prevent play at plate interface during riveting.

5.1.5 Loading

The riveting force used on the quarter FE-model was 0.25*RF, corresponding to force levels applied in truck production at Volvo Group [TR Rivet (2017)]. The loading is applied to the hammer die, Figure 51. During the numerical simulations it is important to apply the correct riveting force in order to obtain realistic results.

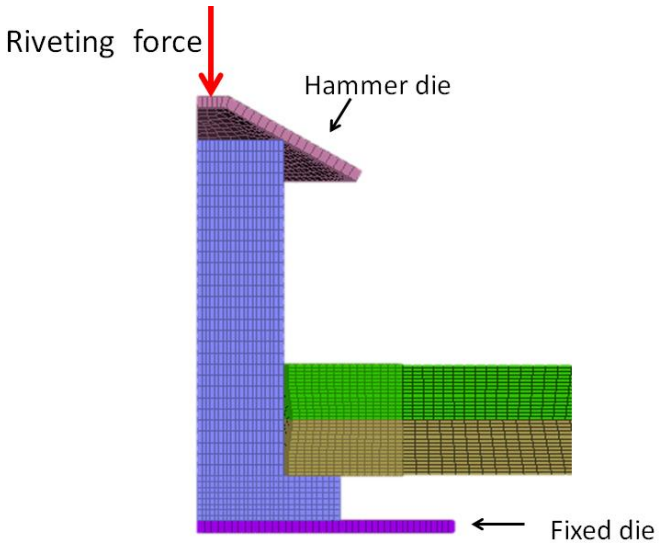

Figure 51 Applied riveting force

In ABAQUS the applied loading can be displacement controlled or force controlled [ABAQUS guide (2014)]. The displacement controlled process is a stable and reliable way of apply loading, but it require an extra step to determine what force correspond to a specific displacement. For the riveting process it is desirable to have a force controlled process as that will allow easy evaluation of different riveting forces, which is convenient as the riveting force is one of the most important design parameters. A stable force controlled loading of the hammer die was obtained when the hammer die was in direct contact with the shank even before the loading was applied, allowing reaction forces to be obtained immediately upon applied load.

5.1.6 Element formulation

A good representation of the stress fields in the simulation is important to evaluate the impact of different design parameters. The element formulation is then important to consider as large deformations occur during the riveting process.

Two different element formulations can be used in ABAQUS, Lagrange element formulation or Eulerian element formulation [ABAQUS guide (2014)]. For a robust simulation when large deformations occurs the Eulerian element formulation is a good choice, but it trades geometric accuracy for the robustness. The Lagrange element formulation is used mainly for small deformations but is still used in this simulation to obtain better geometric accuracy and therefore also a better stress field representations.

5.1.7 Meshing

Using the Lagrange element formulation in the FE-model resulted in large distortions of elements which increase the risk for inaccurate results. Adaptive meshing techniques can then be used to reduce the element distortion and therefore increase the accuracy.

Different adaptive meshing techniques can be used with ABAQUS, adaptive remeshing, mesh-to-mesh or arbitrary Lagrange – Eulerian (ALE) meshing [ABAQUS guide (2014)]. With adaptive remeshing one optimized mesh is found, it requires a lot of computational effort and was therefore disregarded. With mesh-to-mesh the old mesh results are mapped to a new mesh. The technique is mesh dependent with a high risk of discontinuities if there is too large difference between the old mesh and the new mesh, it was therefore also disregarded. With ALE meshing the mesh quality is improved during the simulation as the nodes move independent within the material boundaries. ALE was then chosen as the adaptive meshing technique to improve the mesh quality. Unfortunately it never worked as intended. No apparent difference in mesh could be observed. Different values on the ALE parameters were investigated but no mesh improvement could be observed, Figure 52. Further studies into the ALE meshing method could be made as the mesh quality is reduced using only Lagrange element formulations.

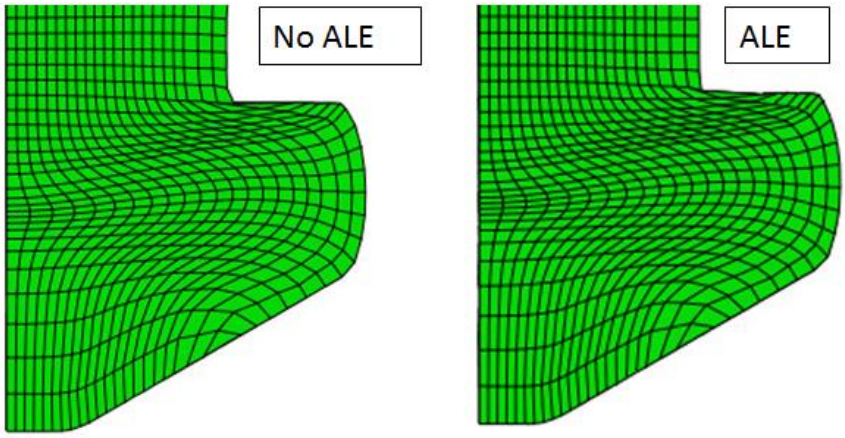

Figure 52 Mesh in shaped rivet head without and with ALE adaptive meshing.

5.1.8 Calculation method

Large deformations and stress transfer between parts occur during riveting and that influence what calculation method can be used. The riveting process is almost a static process [c.f. Huan, H., Liu, M. (2017)] as the riveting force is applied relatively slowly.

In ABAQUS there are three main calculation methods that can be used; static, dynamic implicit or explicit time integration [ABAQUS guide (2014)]. The static calculation method is disregarded as the riveting is not a fully static process. Explicit time integration method is often used to simulate very short processes. It can also be used to simulate longer processes with difficult static or dynamic convergence problems, with the risk of reduced accuracy of the results. Using dynamic implicit method is therefore preferred as possible inertia effects can be considered and high accuracy of results is obtained.

5.1.9 Contact formulation

During the riveting process the rivet shank expands to fill the hole and creates the shaped rivet head. This operation creates difficult contact formulations between the rivet and plates. In ABAQUS there exist different contact formulations depending on what kind of contact there is in the model, the two main formulations are contact pairs and general contact [ABAQUS guide (2014)]. Contact pairs consider the contact between specified surfaces, as the contact surfaces change during the riveting process this formulation was disregarded. General contact formulation with penalty was then used to control contact between surfaces.

During simulation, it was discovered that dynamic implicit calculation method was insufficient for handling the contact situation between the rivet and plates. Convergence of the simulation using dynamic implicit calculation method did not occur even if the contact formulation was supplemented with smoothing and stabilization algorithms. Explicit time integration method was then used instead to avoid problems with the convergence.

The contact formulation was supplemented with an enhanced edge tracking algorithm to ensure a smooth shaped head and good movement around hole edge. A slight adjustment of the edge nodes in the rivet shank was also included to simplify the contact between rivet and hammer die, Figure 53.

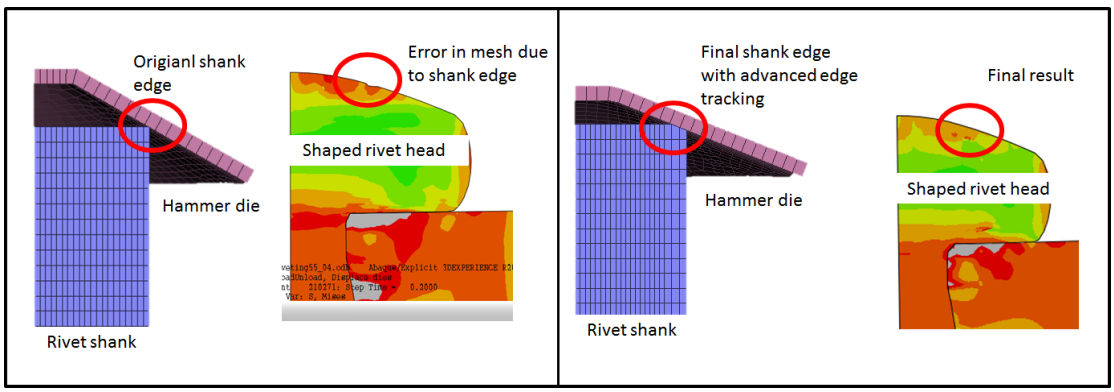

Figure 53 Rivet shank adjustments for good contact formulation.

The friction coefficient was chosen to 0.15 in the simulation to represent general steel surfaces. Chen, N., Ducloux, R., Pecquet, C. et al. (2011) have concluded that the friction coefficient is of less importance during a riveting process, it is therefore not investigated further in this study.

5.1.10 Explicit time integration

Using explicit time integration (ABAQUS explicit) required changes in the simulation model as compared to an ABAQUS implicit model. The explicit time integration method uses much smaller time steps which increase the computational time and therefore also the cost of running the simulation. By manipulating the mass and simulation time of the FE –model the computational time can be reduced.

Depending on if the simulation model is more dynamic or static different guidelines exist for mass and time scaling [ABAQUS guide (2014)]. For static problems with no rate dependent materials the simulated time period can be reduces and the mass of the FE-model can be increased. If rate dependent materials are used reduction of the simulation time should be avoided. For dynamic problems where inertia is important the mass scaling should only be performed for the smallest number of elements possible and reduction of simulation time should be avoided. To verify that the simulation is physically correct after manipulation of mass and simulation time the energy development during the simulation needs to be observed. Kinematic energy should be below 5 % of internal energy. For a static process the total energy should be zero or close to zero compared to the internal energy and for dynamic process the total energy should be constant compared to the internal energy.

As the riveting is close to a static process the mass in the model is increased with 50%, $m_{scaled} = m * 50\%$ were m is the true estimated mass of the model. Only the mass of the smallest elements are additionally increased as needed during the simulation to keep a minimum sized time increment of $t_{inc} = 10^{-6}$ seconds and still allow possible inertia to affect the results. No rate dependent materials are used in this simulation which allowed reduction of simulation time, from $t_{tot} =$ RS to $t_{tot} = 0.2$ seconds. To increase accuracy of the simulated results double precision was used during the calculations. With these settings for explicit time integration the simulation was physically correct when evaluating kinetic, internal and total energy.

5.2 Riveting process evaluation

This section evaluates displacements and residual stresses obtained during the riveting process.

5.2.1 Residual stress fields

The two largest residual stress fields in the plates after the riveting operations are obtained in radial and hoop direction as shown in Figure 54. The shear residual stress from radial and hoop direction will initiate the fatigue cracks. The hoop stress will contribute to the initial widening of the crack. The crack will then propagate through the plate perpendicular to the highest nominal stress. It can also be noted that the residual stress fields are not evenly or symmetrically distributed in plate 1 and plate 2, indicating that the rivet head orientation influence the riveted joint strength.

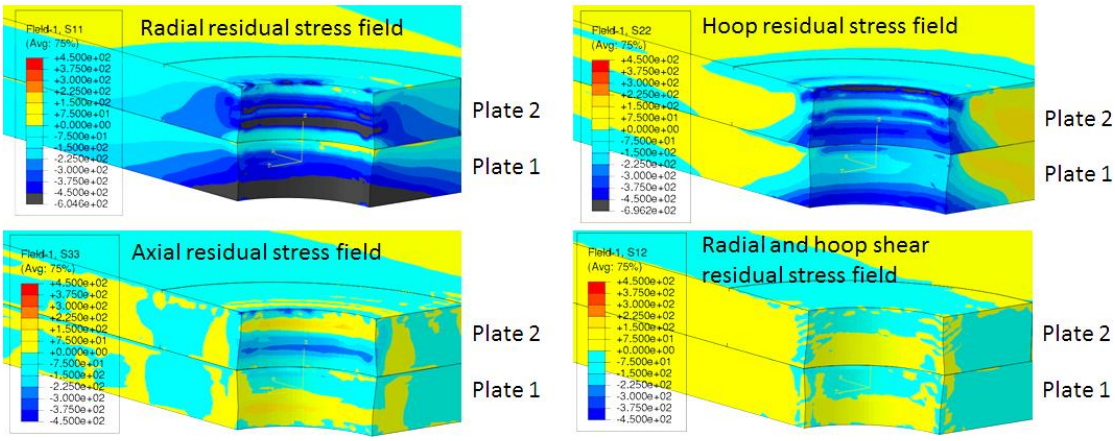

Figure 54 Residual stress fields for convex hole geometry in cylindrical coordinates.

5.2.2 Hole geometry

The hole filling and residual stresses obtained during the riveting process for the different hole geometries; straight, convex, hourglass and stacked is investigated.

The filling of the hole with the different hole geometries are shown in Figure 55. It can be seen that the stacked narrow hole geometry, between plate 1 and the rivet shank, has the largest void, corresponding well with the experimental data. Convex hole geometry experience a very small void while straight and hourglass geometry allow the rivet shank to fill the hole completely.

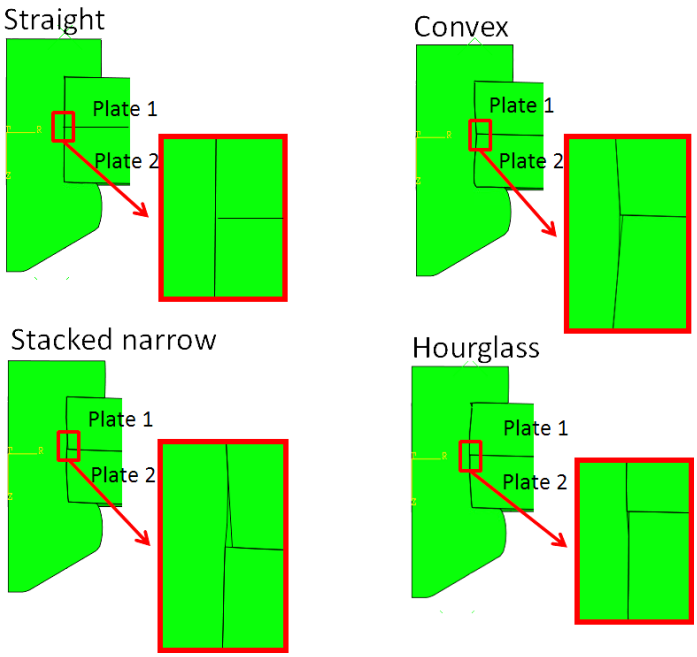

Figure 55 Filling of the hole for the different hole geometries

The residual stress fields are also influenced by the hole geometry, the different hoop residual stresses are shown in Figure 56. Highest tension is identified for the straight hole geometry indicating that this is the worst hole geometry for a long fatigue life as the tension will accelerate crack propagation. The hoop compression observed for the other hole geometries will delay crack propagation.

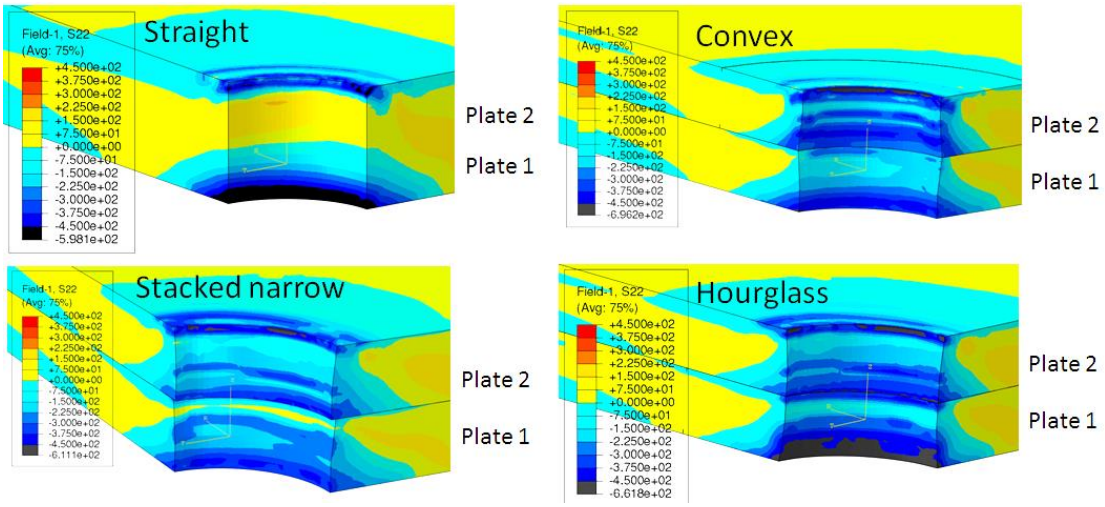

Figure 56 Hoop stress in hole walls for different hole geometries.

5.2.3 Shaped rivet head geometry

The influence of round and flat head geometry is also investigated. The flat head rivet had the free length $L_{free} = 25$ mm and the round head rivet had the free length $L_{free} = 30$ mm. The difference between the rivet head geometries is slight when comparing the residual stress fields of the riveted joint and occurs mainly in the rivet shank, as shown in Figure 57 where the residual stress fields are represented with the Tresca criterion.

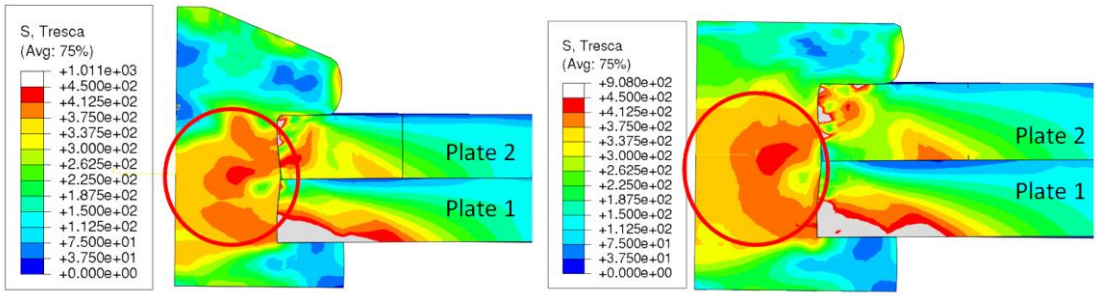

Figure 57 Residual stress field with flat and round shaped rivet head

5.3 Shear loading simulation

In this section a numerical shear loading simulation of a simplified lap riveted joint is described. The goal is to evaluate the stress fields that are obtained during loading of a riveted joint and locate the highest stress range.

5.3.1 FE-model and material model

The FE- model was a simplified version of the riveted joint setup and is shown in Figure 58. The hole was completely cylindrical, straight hole geometry. The rivet was modeled as a pin with two heads laid flush to the plate, no residual stress from the riveting process included. The shaped rivet head was modeled slightly smaller than the factory head to mimic the experimental results.

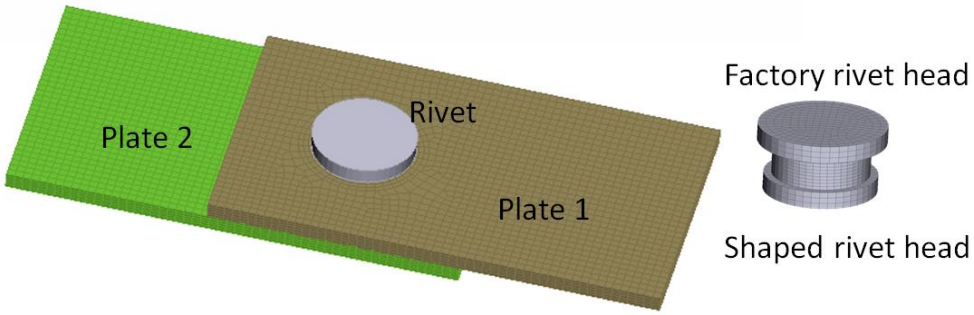

Figure 58 FE- model for shear loading.

The material models for the rivet and the plates are the same as for the riveting process simulation, described in 5.1.2 Material model.

The elements used in the FE-model are the standard solid 3D elements C3D [ABAQUS guide (2014)].

5.3.2 Boundary conditions and loading

The boundary conditions are chosen to mimic the loading that the riveted joints are subjected to during the experiments. One plate edge is fixed while loading is applied at the opposite plate edge of equal distance to the riveted joint as shown in Figure 59.

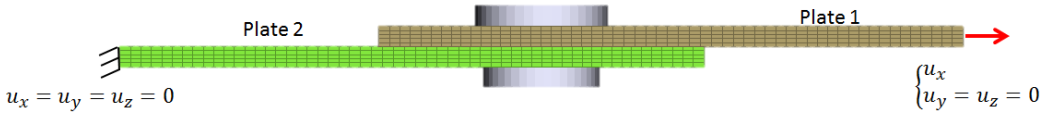

Figure 59 Boundary conditions and loading direction

Two different load cases are simulated as shown in Figure 60, to investigate their influence on the stress fields. For load case 1, the fixed edge and the loading is applied at $L_{plate,loading1} = 105$ mm from the riveted joint. For load case 2, the fixed edge and the loading is applied at $L_{plate,loading2} = 40.5$ mm from the riveted joint.

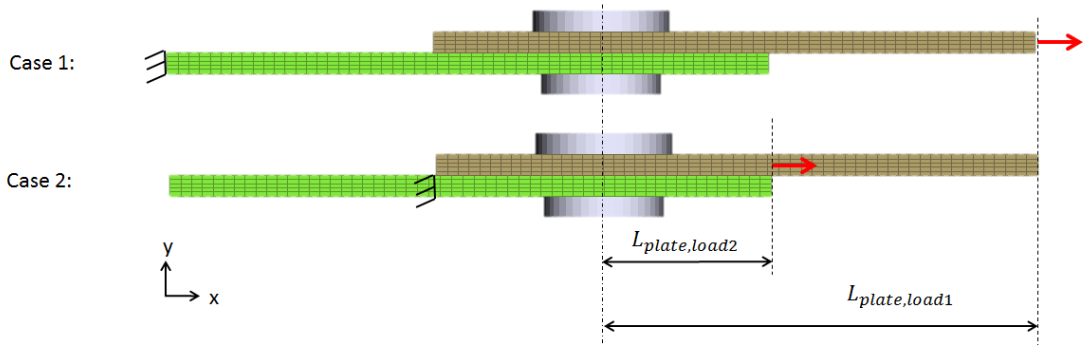

Figure 60 Boundary conditions and loading application for load case 1 and 2.

The applied loading was $= \pm S_{max,L}$, $S = \pm S_{max,M}$ and $S = \pm S_{max,H}$, corresponding to the load amplitudes applied during the experiments. The loading was displacement controlled in ABAQUS to obtain a robust simulation. When computing the displacement no cyclic hardening of the material has been accounted for.

5.3.3 Simulation model

The static calculation method was used to simulate the shear loading. The steel friction coefficient 0.15 was assumed and general contact was specified for all contact surfaces.

5.4 Stress fields

In this section the stress fields obtained during the simulation of shear loading are investigated. The stress field distributions were similar regardless of load level, high tension was obtained at 90 degree to loading and high compression at 0 degree to loading, Figure 61.

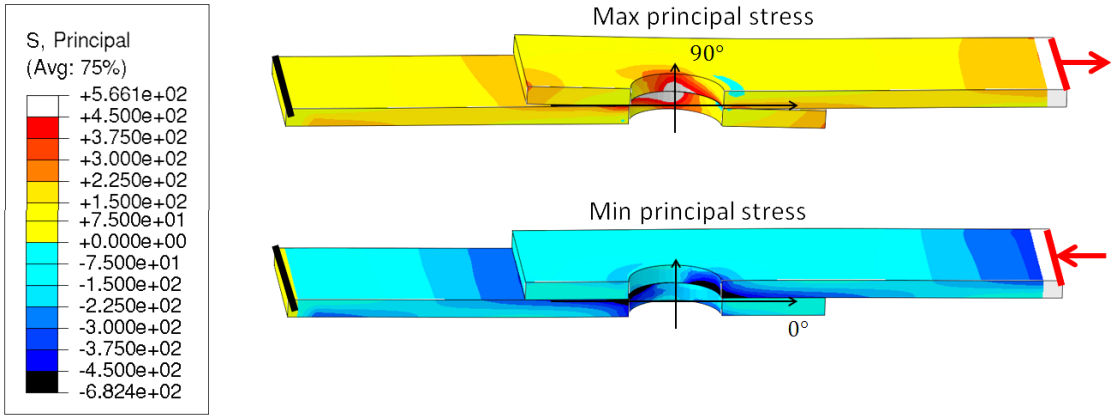

Figure 61 Stress field during shear loading.

The largest stress range, from high tension to low compression was then observed at 45 and 135 degree to loading at the plate interface. The highest stress range for $S = \pm S_{max,H}$ is around 1 000 MPa.

It was noted that the maximum and minim stress levels did not change between load case 1 and 2, the difference was in the size of the stress fields. For load case 2 the stress fields were more concentrated, the highest tension at 90 degree to loading did not stretch as far towards 0 degree as for load case 1, shown in Figure 62. Similar occurred during compression, the compressive stress field were concentrated more around 0 degree to loading compared to load case 1. Load case 2 therefore has a slightly reduced stress range, about 900 MPa, at 45 and 135 degree to loading compared to 1 000 MPa stress range for load case 1.

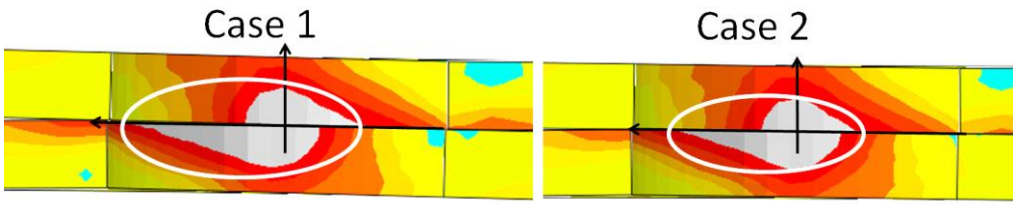

Figure 62 Stress field distribution for load case 1 and load case 2.

5.5 Verification of numerical simulations

The simulation results were compared to the experimental results for verification.

The shaped rivet head geometries are compared in Figure 63. The overall shape of the rivet heads is similar between experiment and simulation, but they differ in height and width. The difference in shape was probably due to the rough estimate of the rivet material model. To gain a better correspondence between simulation and experiments the rivet hardening material model needs to be adjusted. A change of friction coefficient between rivet and plat may also be needed to reduce the shaped rivet head diameter.

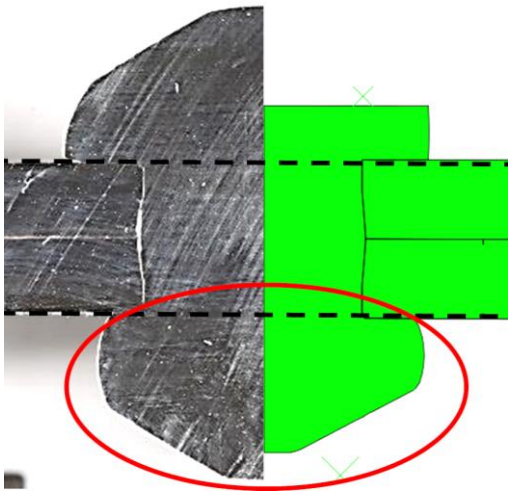

Figure 63 Shaped rivet head geometry.

A good correlation of the hole filling was observed between simulation and experiments, shown in Figure 64.The largest void between rivet and plats were identified for stacked narrow hole geometry, with very small or no identified voids for the other hole geometries.

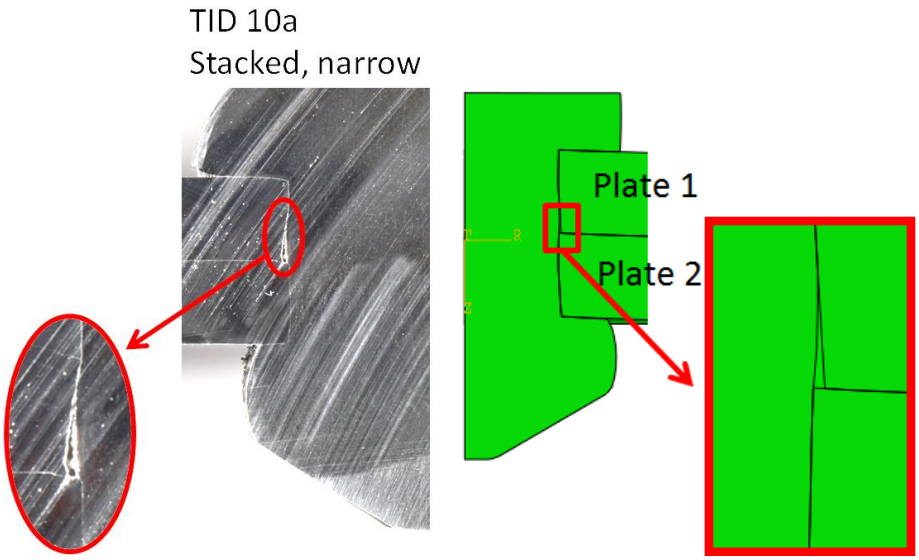

Figure 64 Hole filling. Largest void, between rivet and plates, observed for stacked narrow hole geometry.

The simulated contact pressure on the surface of the rivet shank was compared to the fretting area on a rivet shank, shown in Figure 65. The lower compression in the simulation corresponded well to the fretting area created during experiments.

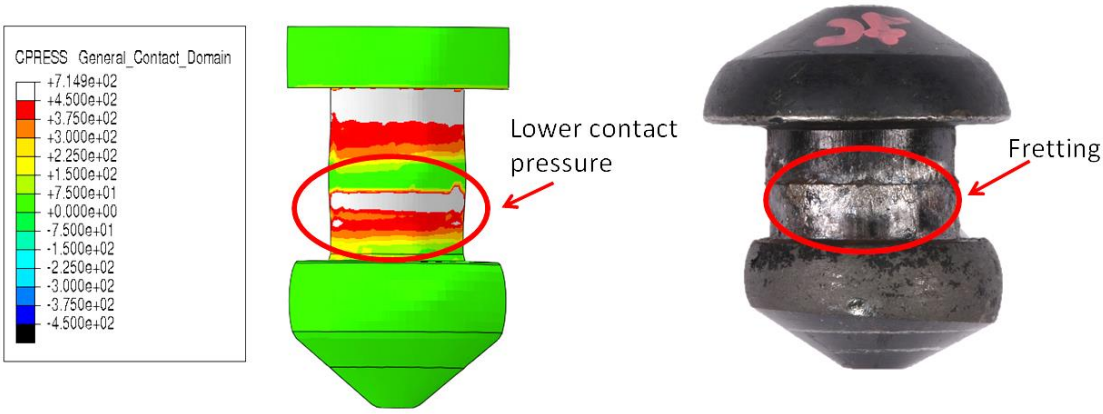

Figure 65 *Simulated contact pressure compared to fretting created during fatigue loading.*

The highest stress range, identified during the shear loading simulation, corresponded well to the crack initiation site during experiments, shown in Figure 66. The critical location was at the plate interface 45 degree to loading direction.

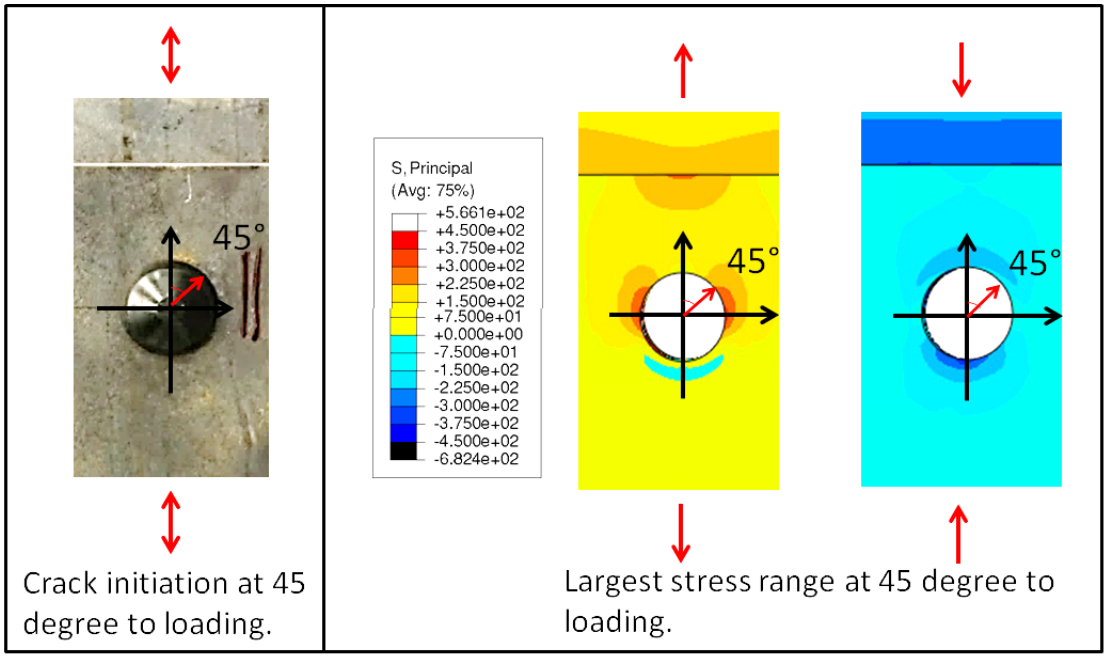

Figure 66 *Crack initiation together with the location of the largest stress range when subjecting the lap joint to shear loading.*

The hole geometry influenced the residual stress fields and also the crack initiation during experiments, shown in Figure 67. Higher tension in the straight hole wall was identified during the riveting simulation. This corresponds to the crack initiations that occurred in the straight hole wall section during experiments.

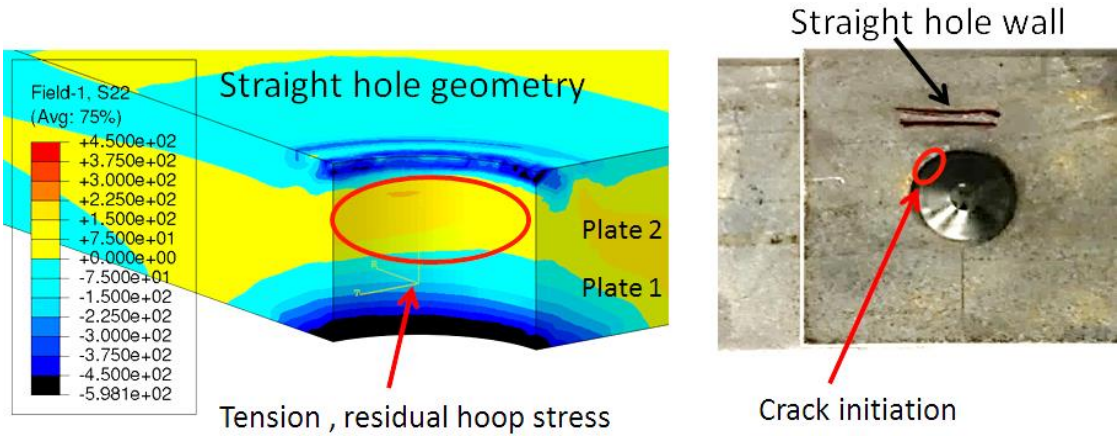

Figure 67 Hoop stress and hole wall geometry comparison.

Crack initiation occurred at the plate interface, in or around the hole wall, during experiments. This corresponded well with the reduced hoop compression obtained around the plate interface during simulation as shown in Figure 68.

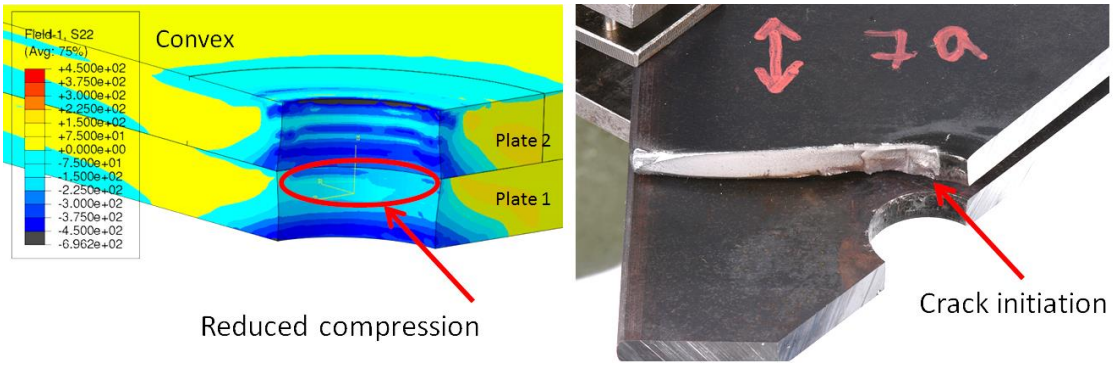

Figure 68 Simulated hoop residual stress field after riveting compared to crack initiation during experiments.

5.6 Error sources

This section describes the possible sources of errors for the numerical simulations.

Material models and geometrical simplifications contribute to errors in the simulation results. The hardening model for the rivet material is a very rough estimate of the true material behaviour and has foremost contributed to the displacement errors in the riveting process simulation. The rivet geometrical shape was simplified to facilitate the meshing. This simplification may have contributed to material flow and material distribution errors.

The quarter symmetrical FE-model used during the riveting process may have induced errors due to the assumption of symmetry. In reality the riveting process is not a completely symmetric process due to rivet placement and existing nominal stress fields in the plates.

Stress field and displacement results are mesh dependent which can induce errors. During the riveting process simulation, large element distortions occur which can induce significant errors in both stress fields and displacement results. An increased

risk for errors arise at sharp corners as the material flow may be hindered due to the mesh and element shape.

Simplifications of stress fields also induced errors. No consideration to residual stress or displacement from the riveting process was considered during the shear loading simulation. This will have induced errors when comparing to the experimental results. Furthermore, cyclic hardening of the steels was not accounted for in the shear loading simulation. This could significantly influence the stress field history during cyclic loading. No regard to residual stresses from hole penetration or plate cutting was included in the riveting process simulation. This could mean that the nominal stress in the plates during simulation is not fully representative of the real nominal stress during the riveting process.

Different restrictions on the plate movements influenced the stress field response during the riveting process simulation as well. Further studies are needed to determine what restriction best represent a real world situation. During this study fixed plate edges were simulated which may have induced amplitude and symmetrical errors in the stress fields.

The riveting dies used in the riveting process simulation were represented as rigid bodies and therefore not allowed any deformation that may occur in a real die. The shape and dimensions of the dies could be further validated against the true dimensions used during industrial production.

The numerical calculation method used during the simulations impact the accuracy of the results. Using the explicit time integration method during the riveting simulation introduced time and mass adjustments. This may have induced stress field and displacement errors. Static calculation method was used during the shear loading simulation and may also have induced errors. The loading was displacement controlled during the shear loading which resulted in errors when comparing the force to the corresponding experimental force.

5.7 Summary of the numerical simulations

This section summarizes the results of the numerical simulations.

The highest residual stress fields in the riveted joint after the riveting process are the radial and hoop residual stresses. The radial and hoop shear residual stress is important to consider as that initiates fatigue cracks. The hoop residual stress is also important to consider as that will widen the initiated crack. With compressive hoop residual stress, the fatigue induced crack initiation could be delayed.

The residual stress fields obtained during the riveting process simulation is influenced by the hole geometry. Straight hole geometry had the highest and largest area of hoop stress tension and is therefore considered as the worst geometry. Stacked narrow hole geometry had small indications of hoop stress tension in the hole wall, but it corresponded to the void obtained between the rivet and plate interface. This might mean that no load transfer during fatigue loading occur at the hoop tension area, improving the riveted joints resistance to crack initiation. Further investigations are need before any final conclusions can be made in that regard. The convex and

hourglass hole geometry only obtained compressive residual hoop stresses in the hole walls, with hourglass geometry obtaining more compression at the plate interface. This indicates that the hourglass hole geometry could be a better performing hole geometry during fatigue loading than the convex hole geometry.

The overall residual stress fields obtained during the riveting process was influenced, not only by the hole geometry, but also by the rivet head geometry. Although, the influence by the rivet head geometry was less than the effect of different hole geometries.

The highest stress range, when subjecting a lap joint to shear loading, was obtained at the plate interface at 45 and 135 degree to loading.

Overall the performance of the simulations corresponded well to the experimental results.

6 Concluding remarks

This section summarizes the findings in this study. The uncertainties in the study are discussed; conclusions drawn and recommendations for future improvements are stated.

6.1 Discussion

The discussion is separated into three sections treating design parameters, experiments and numerical simulations. Some overlap for common discussion points exists.

6.1.1 Design parameters

Much of the data for the literature study was found in studies published by the aviation industry. The studies in the aviation industry mainly investigated lap joints of thin plates held together by a number of small rivets. It is yet undetermined how well this compares to the truck industry where thicker plates and rivets are used. Some design parameters may have a greater influence on smaller riveted joints, other design parameters a greater influence on larger riveted joints. Furthermore, additional design parameters specific for larger riveted joints may also exist that has not been found during this study.

A grading of how influential the design parameters are on fatigue life was difficult to identify during this literature study. This was due to the fact that most studies did not quantify the gain of a specific design parameter. However, the riveting force was the one design parameter that was identified in several studies as having a larger influence on fatigue life. Two studies claimed that cold forming drastically improved the fatigue life. This claim seemed valid as compressive stresses is known to extend fatigue life. It is unknown if other design parameters have a similar drastic improvement of the fatigue life. A good filling of the hole was also one of the overall aspects that was said to improve the fatigue life, but it was not quantified what a good filling actually means. In this study small voids due to incomplete filling were identified during experiments and simulation, no detrimental effect could be observed for these small voids of maximum 1.0 x 0.5 mm during the experiments.

The investigated design parameters were chosen due to availability of material, machines and possible incorporation in industrial truck production at Volvo Group. The riveting force was one parameter that could not be investigated experimentally even if it was identified as a very influential design parameter. Additionally, during previous studies at Volvo Group, the riveting force magnitude for their current riveted joint configuration had already been investigated and was therefore not a priority.

6.1.2 Fatigue life experiments

Uncertainties during the assembly of the riveted joints could possible affect the fatigue life results. One uncertainty was identified during the stamping process, where the punch was not centered over the fixed die. This resulted in an unsymmetrical hole. Where one side of the hole wall was straight while a maximum angled wall was located on the opposite side. During the experiments it was observed that the unsymmetrical hole influenced the crack initiation location. All cracks occurred in the hole wall at the straight hole wall section. This indicates that the limiting hole geometry is the straight hole geometry. This also indicates that the hole geometry that

was intended to be investigated may not have been truly investigated. During the numerical riveting simulations, it could be confirmed that a straight hole wall gave rise to higher tensile hoop stress than any other hole wall geometry investigated. This further confirms that a straight hole geometry is detrimental during fatigue loading.

Due to time constraints a limited number of samples were tested during the experiments, reducing the reliability of the results and the possibility to exclude statistical uncertainties. The overall load amplitude to cycles to failure correspond approximately to similar studies performed by cf., Abdulwahab, F. (2009), Abdulwagab, F. (2010) and Jennfors, P. (1993). The obtained results can then be said to give an indication of possible trends, but further samples need to be investigated to confirm the experimental findings. Notwithstanding, the experimental data can be used for validation of the numerical simulations as shaped rivet head dimensions and crack initiation site were very similar between the different samples.

The large stress range developed in the riveted joint, needs to be considered for fatigue life estimations. During the shear loading simulation it was observed that to move the load application location (the hydraulic grips) the largest stress range of the riveted joint could be manipulated. It is therefore reasonable to assume that a longer fatigue life could be gained by manipulating the load case of the riveted joint to closer resemble only shear loading, as such reducing the largest stress range.

Using cold forming or polishing of the hole should, according to previous studies [cf., Lipski, A. (2012) and Elajrami, M., Miloud, R., Milouki, H., et al. (2016)], result in a significant improvement of the fatigue life. During this study no such results could be confirmed. One reason could be that too high fatigue loads were used. For a continued evaluation of the influence of the hole treatments lower loads should be applied.

Failure mode was in this study load dependent, with clearly different modes for different load amplitudes. The failure modes observed for Abdulwahab, F. (2009) was, on the other hand, dependent on the riveting force. The fractures occurred in the rivet, either at the plate interface or directly below the rivet head. This indicates that the failure mode can be used to determine what design parameters that need to be investigated closer.

A monotonically static load up to $S_{max,Rig}$ was applied to a convex hole geometry without any visible damage. For high amplitude loading during experiments the rivet shank fractured at the plate interface. This indicates that for a riveted joint subjected to high load it is important to have a larger riveted joint. It is therefore possible that the convex hole geometry, that have an increased thickness at the plate interface, would perform better than other hole geometries if the joint is subjected to high loads.

6.1.3 Numerical simulations

The mesh dependence in the riveting process simulation affects the stress fields and displacements results. The critical area was identified at the hole edge in plate 2 directly below the shaped rivet head. The mesh distortion may have prevented material from moving into the hole properly and as such influenced the results. Using adaptive meshing technique in ABAQUS would have been ideal to improve the mesh quality. As stated by Chen, N., Ducloux, R., Pecquet, C. et al. (2011), remeshing is

almost always necessary during the riveting process. The ALE adaptive meshing technique did not, in this study, produce any visibly change in mesh quality.

Another thing that influences the stress field response was the plate restrictions. During the riveting process simulations the plate edges were fixed. This restriction was assumed to best represent that the riveted joint was a small part of a larger structure. This may have induced additional stress levels that did not occur during assembly of the experiments. To clearly represent the plate restrictions it may be necessary to perform further experiments.

The simulation of the riveting process was performed by explicit time-stepping method to manage the difficult contact between rivet and plates. Mass scaling was adopted to reduce computational time, but it also risks reducing the accuracy of the calculated stress fields. With the additional assumption of a quasi-static behavior, time scaling could be utilized to reduce the computational time. The time scaling influence the stress field results and reduces the adaptation of the simulation, preventing the use of rate dependent material models. The residual stress fields in this study are assumed to approximately capture the behavior of the riveting process. Foremost, the residual stress fields should be accurate enough to clearly compare different design parameters as the energy calculations indicate a physically correct simulation model.

The residual stress fields were studied in the riveting process simulation. It was of interest to investigate how the residual stress fields corresponded to the experimental crack initiation and propagation. Fatigue cracks are assumed to initiate in shear, between the two major principal residual stresses [Dowling, N. E. (2013)]. During the riveting process simulation the two major principal residual stresses were obtained as the radial and hoop residual stresses. This leads to the assumption that cracks in a riveted joint should be initiated by radial and hoop shear residual stress, which did correspond to the initial behavior observed during the experiments. Furthermore, the crack propagation during the experiments was then driven by the hoop stress close to the riveted joint. Further from the riveted joint, the crack propagation was driven perpendicular to the nominal stress created by the loading. The crack behavior during experiments and the observed residual stress fields obtained during the riveting process simulation indicates that the hoop stress is critical for the fatigue life. It further indicates that compressive hoop residual stress could delay crack initiation, confirming, among other studies, the Lipski, A. (2012) conclusion that the hoop stress is most important for the fatigue life.

During investigation of the different hole geometries the hoop stress was mainly investigated as that was assumed to be the critical residual stress for a fatigue life assessment. The convex and the hourglass hole geometry obtained only compressive residual stresses in the hole walls. It could therefore be assumed that those hole geometries would give the best fatigue life. The stacked narrow hole geometry obtained some tension in the hole walls. This indicates that this hole geometry would have a reduced fatigue life in comparison to the convex and the hourglass hole geometry. This did not, however, correspond to the experimental results. There the stacked narrow hole geometry gave the longest fatigue life. It is possible that the void, due to bad filling, in the stacked narrow riveted joint actually increased the fatigue life. This would only be possible if the void location corresponded to the tension in

the hole wall and as such prevented load transfer in the area of tension. It is also possible that the experimental results don't really consider the difference in hole geometry as all samples cracked at the straight hole wall and not the hole wall that clearly showed the different hole geometries.

As time did not permit further development of the riveting simulation a shear loading simulation was performed in parallel. The simulation was used to investigate the highest stress range location due to shear loading of a lap joint. As no residual stresses or deformations from the riveting process was accounted for the stress levels cannot be said to correctly correspond to stress levels observed in a real riveted joint. But the simulations seemed to accurately indicate stress field response due to shear loading of a lap joint. As such, the location of the largest stress range could be identified and could also be associated with experimental results.

6.2 Conclusions

Designing a strong riveted joint with a long fatigue life is a balancing act between design parameters. The loading of the riveted joint needs to be considered during design as different characteristics are beneficial at different load amplitudes.

During the literature study three main features were found to influence the fatigue life of a riveted joint; hole filling, residual stress fields and load transfer path. These three features can be manipulated during the riveting process by several different design parameters.

An increased filling of the hole improves the fatigue life. Smaller voids, 1.0 x 0.5 mm at plate interface are acceptable and do not influence fatigue life detrimentally when 15 mm rivets are used.

- **Rivet head design**: Directing material into the hole.
- **Rivet material**: Soft enough to deform and fill the hole without cracking. Strong enough to withstand maximum load in the riveted joint.
- **Radial clearance**: Adjusted to the rivet material hardness.
- **Riveting force**: High enough to compress the rivet.
- **Riveting speed**: Low speed is beneficial as that will reduce heat.

With compressive residual hoop stress and high contact pressure between rivet and plates the fatigue life can be improved. Low nominal stress in the plates can further improve the fatigue life.

- **Rivet head design**: Directing the rivet material and therefore influencing the residual stress fields in the rivet shank and the contact pressure between rivet and plates.
- **Plate material**: Soft enough to deform around the hole, as such obtaining compressive hoop stress in the hole walls.
- **Rivet material**: The rivet material needs to have less spring back than the plate material to form a high enough squeeze force to hold the plates together.
- **Hole penetration method**: Influence residual stress, wall roughness and hole geometry.
- **Hole treatment**: Possible beneficial effects at low loads. For 5 mm thick plates and 15 mm rivets no improvement on fatigue life was observed for medium load, $S_{max,M}$.
- **Hole geometry**: Influences the residual stress fields in the hole walls. Experimental and simulated results in this study indicate that a straight hole wall is detrimental to

fatigue life. Rivet orientation also influence the residual stress fields, higher compression was observed below the factory rivet head.
- **Shaped rivet head dimensions**: Influence residual stress fields, mainly the fields directly below the shaped rivet head.
- **Riveting force**: Just right. As high as possible but not so high that the fatigue life is reduced again.

High or low load amplitude of the riveted joint determines the optimal load transfer path. For high load the majority of the load transfer should be from plate to plate by friction as the plate is of a stronger material than the rivet. For low load amplitudes the majority of the load transfer should be through the rivet as low friction will reduce the possible stress concentration points.
- **Plate material**: Surface roughness influence friction at plate interface.
- **Surface treatment**: Influence surface hardness and roughness.
- **Riveting force**: Influence the squeeze stress.

Additional conclusions can be made regarding fatigue loading of a riveted joint:
- Crack initiation occurs mainly in the hole wall at plate interface either growing from the hole edge into a plate or growing into the rivet.
- For shear loading of a riveted joint the critical crack initiation location is 45 degree to loading.
- Failure mode is load dependent. High loads produce shear failure in the rivet shank. Medium loads produce several small cracks in plate and rivet as the materials give up. Low loads produce one crack that is initiated at a stress concentration point

6.3 Future recommendation

In order to fully optimize the riveted joint it is recommended to further evaluate the different design parameters. It is also recommended to adjust the experimental procedure and the simulation models to increase the reliability and improve accuracy of the results.

The following investigations are recommended per design parameters to increase the knowledge of how the different design parameters influence the riveted joint.
- **Rivet head design**: Investigate how different rivet heads, shank ends and riveting die designs can be used to direct more rivet material into the center of the riveted joint during the riveting process.
- **Rivet and plate material**: Examine the connection between rivet and plate material by studying hardness, strength and spring back. Investigate how low and high strength steel influences the residual stress field after riveting, primarily how it influences the fatigue life at low loads. Investigate also the, possible, connection between the rivet diameter and the plate thickness. Furthermore, investigate how the plate rolling direction and loading direction can influence the fatigue life.
- **Surface treatment**: Investigate which surface treatments, in correlation to load level, produce a better fatigue life. Furthermore, investigate what friction is beneficial at what load level.
- **Radial clearance**: Investigate the needed radial clearance for different rivet and plate materials to create a sufficiently strong riveted joint.

- **Hole penetration method**: Investigate the effect of different penetration methods on the fatigue life.
- **Hole treatment**: Investigate different hole treatments at low loads. Examine how surface roughness and the residual stress in the hole walls influence the fatigue life.
- **Hole geometry:** Investigate the fatigue life at low loads for different hole geometries where the hole walls are symmetric. Furthermore, investigate the influence of factory rivet head orientation.
- **Shaped rivet head dimensions**: Investigate how riveting die design together with the design of the shank end can improve strength of the riveted joint. Also of interest is to investigate how to reduce the free length of the rivet shank while improving the fatigue life.
- **Riveting force**: Examine how the hoop and squeeze residual stress corresponds to the riveting force. Furthermore, investigate what riveting force in combination with plate and rivet material is needed to obtain a good fatigue life. Additionally, also investigate at what level the riveting force becomes detrimental to fatigue life.
- **Riveting speed**: Investigate at what speed, in combination with rivet material, that the riveting process should be performed with to produce an optimal fatigue life of the riveted joint.

The following recommendations are made to improve reliability and accuracy of the results when performing experiments.

1. Increase the accuracy when producing the test specimens by calibrating needed machines and using assembly rigs.
2. Reduce bending in the riveted joint to improve the fatigue life estimates for shear loading. The reduction could be achieved by moving the hydraulic grips of the test rig closer to the center of the riveted joint.
3. Use at least three samples per investigated parameter and load level to gain statistical reliable results.

The following recommendations are made to improve the accuracy of the numerical simulations.

1. The hardening material model for the rivet needs to be adjusted to improve correlation to experimental data. The rivet material deformed more during the riveting simulation than during the experiments. This indicates a too soft hardening material model for the rivet.
2. Mesh distortion should be reduced to improve the accuracy of the simulation. Continue the investigation of how remeshing techniques can be used during the riveting process to improve the mesh quality.
3. Mesh convergence should be investigated to verify the stability and the reliability of the simulations.
4. No cyclic loading has been accounting for when simulating the shear loading. It is therefore recommended to add cyclic material data for further evaluations of how shear loading influence the riveted joint
5. Plate restrictions during the riveting process needs to be investigated further to improve correlation to experimental behavior. Investigate experimentally, the stress - strain field at the plate surface around the riveted joint, with the use of a strain gauge. Compare the results to the corresponding stress fields obtained during the riveting simulation.

6. The contact formulation in the riveting simulation needs to be improved to create smoother stress fields in contact areas between rivet and plates.
7. Energy convergence should be investigated to verify that a stable and reliable riveting process simulation has been obtained when mass and time scaling is used.

The following implementations are recommended for expanding the use of the simulation models.

1. Include residual stress fields obtained during the hole penetration to improve accuracy of the residual stress fields obtained during the riveting process simulation.
2. Add material rate dependency to the riveting process simulation to improve the material behavior. Rate dependent material is necessary for investigation of the influence of riveting speed on the riveted joint. Adjust time scaling as necessary.
3. Include heat dependent material data during the riveting process to simulate heat dependence, correlate to experimental temperature measurements. Adjust time scaling and element type as needed.
4. Expand the riveting simulation to encompass shear loading of the riveted joint.
5. Add cyclic plasticity models to be able to simulate fatigue loading of a riveted joint, conduct experiments as necessary.
6. For an improved fatigue life assessment consideration should be taken to the changing friction coefficient, especially at the plate interface where the friction response depend on fretting development during cyclic loading.

7 References

ABAQUS (2017): ABAQUS 3DEXPERIENCE R2017X. Dassault Systèmes, https://www.3ds.com

ABAQUS guide (2014): ABAQUS 6.14 Online Documentation, 2014.

Abdulwahab, F. (2009): ER- 700200. Volvo Powertrain Corporation, 2009.

Abdulwagab, F. (2010): ER- 701235. Volvo Powertrain Corporation, 2010.

ANSA (2018): ANSA version 18.0.1. BETA simulation solutions, https://www.beta-cae.com/ansa.htm

Baha II, S., Hesebeck, O. (2010): Simulation of the Solid Rivet Installation Process. *SAE International Journal of Aerospace.*Vol 3, No 1, 2010, pp. 187-197.

Chen, N., Ducloux, R., Pecquet, C., Malrieux, J., Thonnerieux, M., Wan, M., Chenot, J. L. (2011): Numerical and experimental studies of the riveting process. *International journal of material forming,* Vol 4, No 1, 2011, pp 45-54.

Dowling, N. E. (2013): *Mechanical behavior of materials Engineering methods for deformation, fracture, and fatigue*. Essex: Pearson education Limited, 2013.

Elajrami, M., Miloud, R., Milouki, H., Boukhoulda, F. B. (2016): Experimental investigation of the effect of double cold expansion on the residual stress distribution and on the fatigue life of rivet hole. *Journal of the Brazilian society of Mechanical Science and Engineering*, Vol 38, No 8, 2016, pp 2527-2532.

Fuiorea, I., Bartis, D., Nedelcu, R. (2009): The rivet parameter influence in fatigue strength. *Fatigue of aircraft structures*, Vol 1, 2009, pp 50-57.

Huan, H., Liu, M. (2017): Effects of squeeze force on static behavior of riveted lap joints. *Advances in Mechanical Engineering* Vol 9, 2017, pp 1-13

Jennfors, P. (1993): ER- 212504. Volvo Truck Corporation, 1993.

Kaifu, Z., Hui, C., Yuan, L. (2011): Riveting process modeling and simulating for deformation analysis of aircraft's thin-walled sheet-metal parts. *Chinese Journal of Aeronautics,* Vol 24, No 3, 2011, pp. 369-377.

Klintman, S. (2018): Personal communication 2018. SSAB, https://www.ssab.com/.

Lacroix, D. (2016): ER- 708724. Volvo Material technology, 2016.

Lipski, A. (2012): The influence of the degree of the rivet hole sizing on the fatigue life. *The journal of institute of aviation* Vol 1, No 4, 2012, pp 64-69.

Ottosen, N., Petersson, H.(1992): *Introduction to the finite element method*, Prentice-Hall, Harlow, 1992.

Ragot, S (2018): Personal communication 2018. Volvo GTT.

Sandström, B. (1993): ER- 500215, Volvo, 1993.

Skorupa, M., Skorupa, A., Machniewicz, T., Korbel., A. (2010): Effect of production variables on the fatigue behavior of riveted lap joints. *International journal of fatigue* Vol 32, No 7, 2010, pp 996-1003.

Skorupa, M., Machniewicz, T, Skorupa, A., Schijve. J., Korbel. A. (2015): Fatigue life prediction model for riveted lap joints. *Engineering Failure Analysis*, Vol 53, 2015, pp. 111-123.

Skorupa, M., Skorupa, A., Machniewicz, T., Korbel. A. (2016): Effect of load transfer by friction on the fatigue behaviour of riveted lap joints. *International journal of fatigue* Vol 90, 2016, pp 1-11.

TR Rivet (2017): *Technical requirements for rivet*, Document No 1579857, Volvo group truck technology, 2017.

Volvo Group (2018): Volvo Group, https://www.volvogroup.com/.

Zarabi, R. (2005): Er 506587. Volvo Truck Corporation, 2005.